A STUDY OF NOVEL ACTIVITIES OF TYPE III SIRTUINS: COBB AND PFSIR2A

A Dissertation

Presented to the Faculty of the Graduate School

of Cornell University

in Partial Fulfillment of the Requirements for the Degree of

Doctor of Philosophy

By

Anita Y Zhu

August 2013

A STUDY OF NOVEL ACTIVITIES OF TYPE III SIRTUINS: COBB AND PFSIR2A

Anita Y Zhu, Ph.D.

Cornell University 2013

Sirtuins are a class of nicotinamide adenine dinucleotides (NAD)-dependent histone deacetylases (HDACs) found in all three domains of life. Acetylation-deacetylation of histones lysine residues is an accepted paradigm for gene regulation in eukaryotes. In recent years, proteonomic studies revealed that many cellular proteins are acetylated and are regulated by post translational modifications. Although initially, sirtuins gained notoriety when Sir2 yeast was discovered to increase life span under calorie restriction, current research suggests that sirtuins are involved in a myriad of other cellular functions. The discovery of Sirt5's, a type III mammalian sirtuin,novel desuccinylase/demalonylase activity opened up new possibilities of cellular protein regulation. Two conserved active site residues, Tyr and Arg, are believed to be responsible for Sirt5's desuccinylase/demalonylase activity. The physiological importance of lysine succinylation and malonylation is strengthened by proteonomic studies that have identified succinylated and malonylated proteins. Many of those proteins are involved in metabolism and gene regulation suggesting that Sirt5 is important.

Our aim was to verify the importance of the two conserved residues in type III sirtuins and investigate the physiological significance of these new post translational modifications in a bacterial model. We investigated the activity of two sirtuins, *E. coli* CobB, bears the two active site residues, and *Plasmodium falciparum* Sir2A (PfSir2A), a type III sirtuin missing the conserved residues, and found that only CobB has desuccinylase activity while PfSir2A prefers

to remove long fatty acyl chains. We followed up on the physiological relevance of lysine succinylation by screening for CobB substrates in *E. coli* and found that CobB can regulate RcsB's DNA binding capability by lysine desuccinylation. We also investigated CobB's influence on metabolism in different nutrient conditions and found that desuccinylation was not important in acetate, succinate and propionate supplemented nutrients.

BIOGRAPHICAL SKETCH

Anita Yuhua Zhu graduated with a Bachelors of Science degree in Biomolecular Sciences from Polytechnic Institute of New York University with honors and earned her Masters of Science degree in Biomedical Engineering the following year at the same institute. During her Undergraduate and graduate career at Polytechnic, she worked under the supervision of Dr. Jin Kim Montclare on the positional effects of incorporating fluorinated phenylalanines into histone acetyltransferases which won the Roland Ward's Best Undergraduate Thesis Award. In August 2008, she started her graduate career at Cornell University and eventually joined Dr. Hening Lin's lab to study the novel enzymatic activities of bacterial sirtuins - CobB and PfSir2A. From 2009-2011 she was a Chemistry and Biology interface grant trainee who completed an internship at L'Oreal USA.

To my mother and grandmother,

Caring and patient,

In rain or shine.

ACKNOWLEDGEMENTS

I like to thank my advisor Dr. Hening Lin first and foremost for his support and encouragement in life and science. There were many times that my research seemed like a meandering road and without Hening's guidance I would have been truly lost. I also like to thank my committee members Dr. Steve Ealick and Dr. Richard Cerione for being there to critique my research and urge me to better myself as a scientist.

I would also like to thank all the members of the Lin Lab, past and present, for making what seemed like endless days of research fun – especially Xiaoyang Su, who taught me the basics of molecular biology techniques and the voice of reason when life spun out of control; Jing Hu, Min Dong, and Colleen Kummel, who always had time to lend a helping hand no matter the time of day; Kenny Kang and Yoon Ha Cha, who were nice enough to lend me a helping hand in research when two weren't enough; Jintang Du, who being my first mentor in a new lab; Hong Jiang, Bin He, Jonathan Harold Shrimp and Zhewang Lin, who indulged my nervous baking habits by eating all the sweets.

Last but not least, I like to thank NIH for providing funding that made research possible, with an especial thanks to the CBI training grant for giving me the opportunity to focus on research; our collaborator Yeyun Zhou for solving the crystal structure of PfSir2A with H3K9 Myristoyl peptide; Yale's *E. coli* genomic stock center for providing CobB parent and Knockout strains; NBRP-*E.coli* at NIG for providing free strains for research.

TABLE OF CONTENTS

LIST OF FIGURES

LIST OF TABLES

CHAPTER 1: BRIEF OVERVIEW OF MAMMALIAN SIRTUINS AND THE FUNCTION OF DEACETYLATION AND ACETYLATION IN BACTERIAL CELLS

ABSTRACT

Sirtuins are nicotinamide adenine dinucleotide (NAD)-dependent deacetylases. When it was discovered that Sir2 in yeast can promote longevity in conjunction with calorie restriction, sirtuins garnered significant attention. Since then, the study of sirtuins have revealed a myriad of functions spanning from metabolism, cancer, stress and chromatin regulation in addition to healthspan. Mammals have 7 sirtuins, Sirt1-7, that were designated with deacetylase activity. Lysine deacetylation and acetylation has been well studied on histones and non-histones proteins in mammalian cells. However, in bacteria the purpose of this lysine acetylation and deacetylation paradigm is still largely unknown due to lack of research. Here we will review the function of lysine acetylation in bacteria and how sirtuins are involved.

INTRODUCTION

Sirtuins are a class of histone deacetylases (HDACs) that needs nicotinamide adenine dinucleotide (NAD) as a co-substrate to function. They are found in all three domains of life, bacteria, archaea and eukaryote. The most complex organism can have up to 7 sirtuins, as seen in humans, while bacteria such as *S. enterica* and *E. coli* have only one[1]. A phylogenetic study of sirtuins by sequence alignment classified them into 5 types: I, II, III, IV and U. A popular model for the evolution of of sirtuins in eukaryotes is that the first eukaryote received its sirtuins from the engulfment of an α-proteobacterium by an archaean which supplemented a type II and U and type III sirtuins, respectively. Since type I and IV have the greatest sequence similarity to type U, it is most likely that type I and IV sirtuins evolved from type U (Fig.1) [2].

Mammals have 7 sirtuins (Sirt1-Sirt7) which encompasses the four major types of sirtuins (I-IV) [1]. Sirt1 to Sirt3 are type I sirtuins, Sirt4 belongs to type II sirtuins, Sirt5 is a type III sirtuin and Sirt6 and Sirt7 are type IV sirtuins. Sirt1-7 are localized differently in the cell and expression levels are tissue dependent [3]. Sirt1, Sirt6 and Sirt7 are localized primarily in the nucleus, Sirt2 is mainly a cytosolic enzyme and Sirt3, Sirt4 and Sirt5 are localized in the mitochondria[4]. The type I sirtuins have robust deacetylation activity, while type II to type IV have very weak to no deacetylase activity [4]. Although reports suggested that some of these sirtuins could be ADP-ribosyltransferases [5], our data and that from Denu and coworkers suggest that the ADP-ribosyltransferase activity of sirtuins is very weak and unlikely to be physiologically relevant [6, 7].

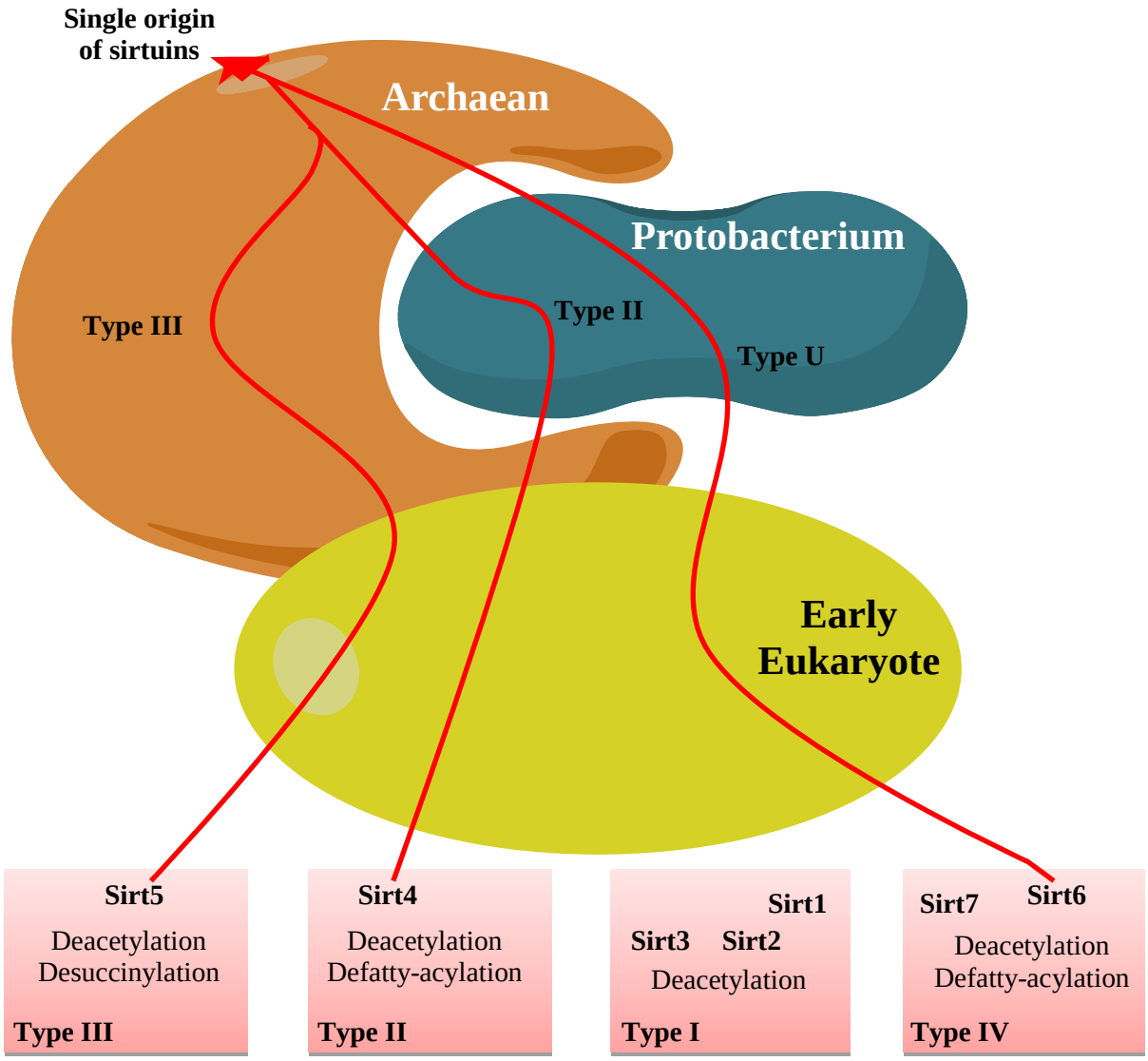

Figure 1. Evolution of sirtuins. There are 5 types of sirtuins, I-IV and U, and each type has a characteristic function. A popular model for the evolution of sirtuins in the first eukaryote is that the parent archaean, which carried type III already, engulfed a protobacterium that carried type II and type U sirtuins. Eventually type I and IV sirtuins evolved from type U sirtuins. Mammals have 7 sirtuins, Sirt1-7. Sirt1-3 are type I sirtuins that each exhibits robust deacetylase activity. Sirt4 is a type II sirtuin which exhibits a weak deacetylation activity and may function as a defatty-acylase. The exact functions and enzymatic mechanism are still unknown. Sirt5 is a type III sirtuin that also has weak deacetylase activity, but has recently been found to be a strong desuccinylase/demalonylase. Sirt6 has made some strides recently as a deacetylase, however, its deacetylase activity is relatively weak when compared to its demyristoylation activity. While Sirt7 is still a mystery, we can hypothesize that since it is in the same class as Sirt6, it is most likely a long chain defatty-acylase. Figure adapted from [8] .

THE EFFECT OF (PTMS) ACETYLATION AND DEACETYLATION ON LYSINE RESIDUES IN BACTERIA

Lysine acetylation of histones established the importance of gene regulation by post-translational modifications, but later proteomics studies discovered that non-histone proteins were also lysine acetylated suggesting that lysine acetylation may be involved in many eukaryotic cell processes[9, 10]. The two separate proteomics studies found hundreds of acetylated lysine residues on as many as 91 *E. coli* proteins[9, 10]. While the proteins identified in both studies contained similar proteins only the lysine residues listed in Table 1 were identified in both studies. The majority of the modified proteins were metabolic enzymes and translation regulators[9, 10]. The array of proteins found to be acetylated in *E. coli* indicates that this modification is a highly abundant and evolutionarily conserved post translational modification found in diverse functions of life[9, 10].

Many bacterial proteins have confirmed functions regulated by acetylation. Acetyl-coenzyme A synthetase (ACS), CheY, and RcsB have been identified and experimentally determined to be regulated by the acetylation/deacetylation of targeted lysine residues[11, 12]. ACS can catalyze the production of acetyl-CoA from acetate and coenzyme A in an ATP driven reaction[11]. The acetylation of a highly conserved lysine residue (lys609) blocks the adenylation of acetate, and hence the production of acetyl-CoA[11]. This example highlights the importance of acetylation/deacetylation in bacterials cells because acetyl-CoA is at the core of central metabolism. Interestingly enough activated ACS can acetylate CheY, a chemotaxis regulator[12]. It has been found that upon acetylation of a lysine residue cluster, CheY loses its ability to bind CheA, CheZ and FliM and hence its chemotactic abilities[12]. This was later found to be part of a slow mode of regulation dictated by the metabolic state of the cells[12]. A

fast mode of regulation is mediated by phosphorylation of CheY, with CheA as the phosphor donor[12]. While CheY can be auto-acetylated with acetyl-coA as a donor, Δ*acs* mutants exhibit defective chemotactic responses[12]. Thus, this rules out any significant effect that auto-acetylation may have in regulation of CheY and at the same time supports that the acetylation of CheY by ACS may likely be apart of an acetylation cascade[13].

Table 1. Lysine-acetylated proteins identified from two independent studies. Only 8 of the proteins had the same acetylated peptides identified in both experiments. Extracted from [9, 10].

Gene	Protein Name	GI No.	Functional Classification	Shared Peptide Sequence
gltA	Citrate Synthase	gi|16128695	TCA Cycle	MLEEISSV**K**HIPEFVR
ICD	Isocitrate Dehydrogenase	gi|2618886	TCA Cycle	YYQGTPSPV**K**HPELTD MVIFR
aceE	Pyruvate Dehydrogenase Complex, Dehydrogenase Component (E1)	gi|83584560	TCA Cycle	
aceF	Dihydrolipoamide Acyltransferase (E2)	gi|75258892	TCA Cycle	VDFS**K**FGEIEEVELGR
ipd	Dihydrolipoamide Dehydrogenase (E3)	gi|26106453	TCA Cycle	DIV**K**VFTK
pgi	Phosphoglucose Isomerase	gi|68304110	Glycolysis	
eno	Enolase	gi|563868	Glycolysis	
ytjC	Phosphoglyceromutase	gi|13360242	Glycolysis	AETAE**K**YGDEQVK HYGALQGLN**K**AETAEK
gapA	Glyceraldehyde-3-phosphate Dehydrogenase	gi|37699654	Glycolysis	DNTPMFV**K**GANFDK TVDGPSH**K**DWR
tktB	Transketolase	gi|75227108	Carbohydrate Metabolism	
rpsF	30S Ribosomal Protein S6	gi|133976	Ribosome	
fusA	Elongation Factor G	gi|110643581	Translation	
tufA, B	Elongation Factor Tu	gi|26249935	Translation	FESEVYILS**K**DEGGR
tnaA	Tryptophanase	gi|41936	Amino Acid Metabolism	GAEQIYIPVLI**K**K MENF**K**HLPEPFR NVYI**K**EAFDTGVR
pepD	Aminoacyl-histidine Dipeptidase	gi|26246281	Protein Metabolism	
ahpC	Alkyl Hydroperoxide Reductase, C22 Subunit	gi|1786822	Oxidative Stress Response	
groL	GroEL	gi|99867128	Chaperone	
guaB	IMP Dehydrogenase	gi|146275	Nucleotide Metabolism	

Another recent paper studying acetylation discovered that gene regulation in bacteria may also be regulated by acetylation/deacetylation[14]. The paper identified that RcsB, a transcription regulator that mediates many cellular processes such as cell division, motility, osmotic responses and capsule biosynthesis can be deacetylated at lys140 by CobB[14]. Deacetylation of RcsB activates its ability to bind DNA, specifically the binding of *flhCD* operator sequence[14]. This

was the first paper to demonstrate that like eukarotyes, bacterial transcription is also regulated by acetylation/deactylation[14]. The involvement of sirtuins in the deacetylation of lysines have demonstrated the importance of acetylation in the regulation of metabolism and gene regulation in mammals.

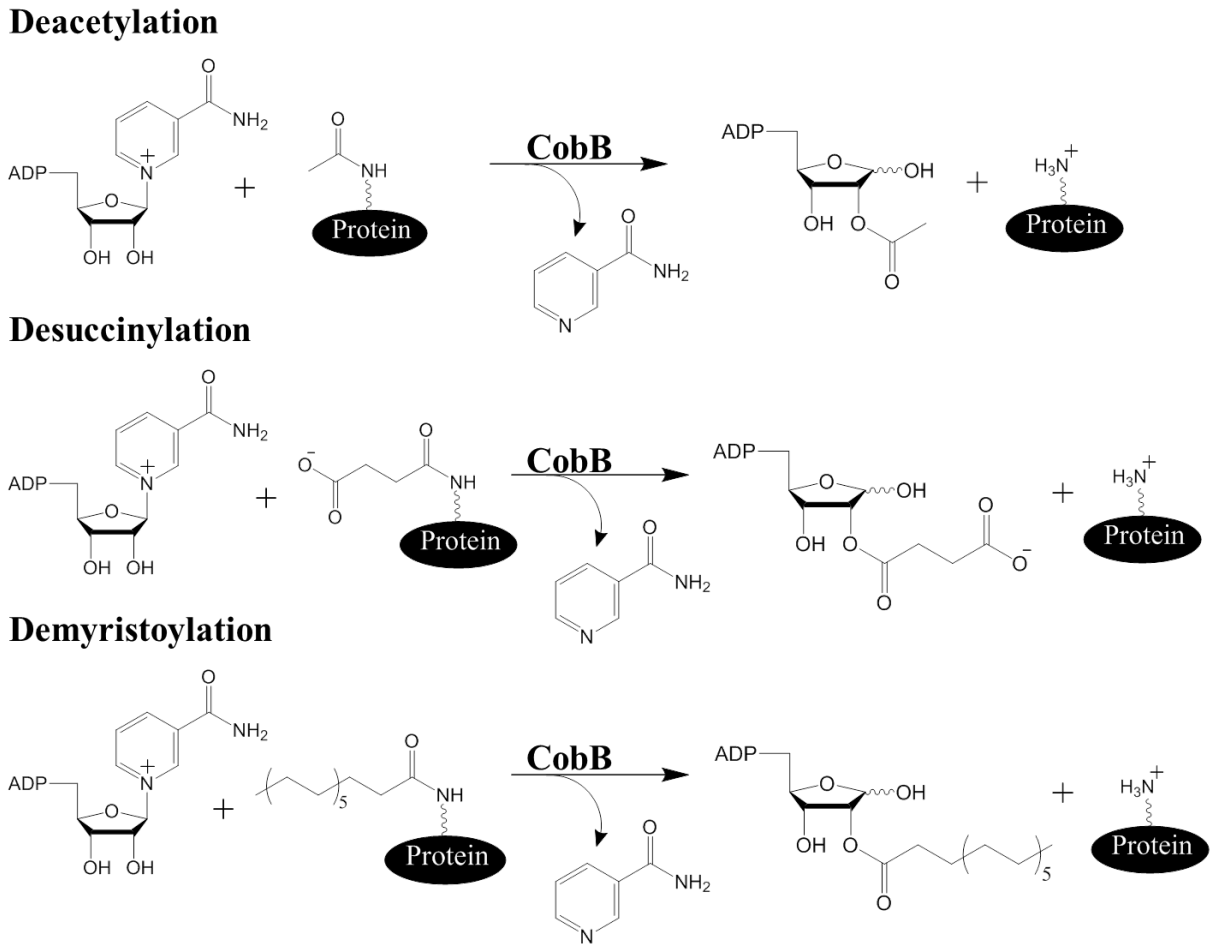

Figure 2. Deacylation of lysine residues catalyzed by CobB.

There are two main enzymes that have been identified as the regulators of acetylation/deacetylation paradigm in bacterial cells. PAT, protein acetyl transferase, in most cases acetylates lysine residues while, CobB, an NAD dependent sirtuin catalyzes the deacetylation of lysines[11]. CobB is the only known bacterial sirtuin in *S. enterica* and *E. coli*

and it is a type III sirtuin similar to that of Sirt5 found in humans. We determined experimentally that CobB is a multifunctional enzyme that carries many activities (figure 2). Through an *in vitro* screen with various lysine acylated H3K9WW peptides, we determined that CobB has a strong activity for acetylated, succinylated and myristoylated lysine residues.

In Chapter 2, we will further discuss CobB's enzymatic activity and how those functions help regulate cellular functions. The identification of succinylated lysine residues across species in a proteomics study suggests that succinylation/desucccinylation may be another paradigm that is important for cellular regulation in eukaryotes as well as prokaryotes. Since CobB is multifunctional, it is important to investigate the singular and combination effect that its activities may have downstream on its substrates and processes. This new discovery also shows us how intricate the web of posttranslational modifications is in cells. In the following chapters we will investigate two type III proteins that both exhibit novel sirtuin activities and the role these sirtuins play in cellular function.

CHAPTER 2: COBB IS A PROMISCUOUS SIRTUIN

ABSTRACT

Sirtuins are traditionally known as nicotinamide adenine dinucleotide (NAD) –dependent deacetylases and they exist in all three domains of life. Many bacterial sirtuins such as CobB in *E. coli* and *S. enterica* have the greatest sequence homology to Sirt5, a type III sirtuin. Recent discovery of Sirt5's desuccinylase/demalonylase activity has opened up possibilities of a new paradigm. Two residues, Arg and Tyr, found in most type III sirtuins are responsible for Sirt5's lysine malonyl/succinyl activity. These observations prompted us to examine whether all type III bacterial sirtuins, specifically *E. coli* CobB, can catalyze demalonylation or desuccinylation. Previously CobB has been reported to regulate metabolism in *S. enterica* when it upregulates the activity of acetyl-CoA synthetase (ACS) by lysine deacetylation. CobB has also demonstrated gene regulatory capabilities with *E. coli* RcsB, a transcription factor responsible for a complex signal transduction network. We have found that *E. coli.* CobB is a multifunctional enzyme with robust deacetylase as well as desuccinylase activity. We investigated CobB's desuccinylation activity in regards to metabolism and gene regulation and have found that while there appears to be no significant affect to metabolism, desuccinylation is important for the DNA-binding capabilities of RcsB. Our investigation shows that it is desuccinylation of RcsB rather than deacetylation that increases DNA binding.

INTRODUCTION

Sirtuins are a class of HDACs known as nicotinamide adenine dinucleotide (NAD)-dependent deacetylases [1]. About half of the mammalian sirtuins have very weak or no deacetylase activity in vitro [15]. Recently, we discovered that human Sirt5, a type III mitochondrial sirtuin that has weak deacetylase activity, can catalyze the hydrolysis of malonyl and succinyl lysine peptides much more efficiently than the hydrolysis of acetyl lysine peptides [16]. Furthermore, mammalian proteins were found to contain malonyl and succinyl lysine modifications [16]. The recognition of malonyl and succinyl groups by Sirt5 is determined by the presence of an arginine and tyrosine residue in the active site [16]. The arginine and tyrosine residues are conserved in most type III sirtuins, including *E. coli* CobB. Here we report that *E. coli* CobB, similar to Sirt5 can catalyze the hydrolysis of succinyl lysine efficiently. However, different from Sirt5, the deacetylase activity of CobB is also very efficient, suggesting that *E. coli* CobB is a multifunctional sirtuin. Furthermore, we found that succinyl lysine is also present in *E. coli* proteins. More succinyl peptides were identified from a CobB deficient strain, suggesting that CobB controls the succinylation level in *E. coli*. Given that succinylated proteins are involved in a myriad of functions in the cell, from DNA regulation to metabolism, we investigate the relevance of lysine succinylation in *E. coli*.

Metabolism is required for the survival and proper function of all living cells. Posttranslational modifications of metabolic enzymes have been increasingly recognized as important means of regulating metabolism [17]. Recent proteomic studies revealed that many metabolic enzymes are acetylated on lysine residues and acetylation-deacetylation regulates the activity of the metabolic enzymes in response to nutrient conditions, in both mammals and bacteria [18, 19] . We wondered if the same is true about succinylation-desuccinylation and

studied the relevance of CobB and R95M, a mutant of CobB deficient in desuccinylase activity, in a *ΔcobB E. coli* strain under different nutrient conditions. While we identified several succinylated metabolic proteins, we could not establish the physiological relevance of this novel PTM.

Post-translational modifications on histones has been a widely accepted concept that is important in gene regulation [20, 21]. The model of histone acetylation-deacetylation is especially important for the DNA transcription. While this model has been established in many Eukaryotic organisms, in bacteria it is still a fairly new concept. Recently, it was reported that RcsB, a transcription factor, is regulated by CobB and protein acyltransferase (PAT) [14]. The acetylation-deacetylation of Lys180 affected the DNA binding capability of RcsB which affected the expression of *fhDC* genes that positively regulates flagellum biosynthesis [14]. CobB deacetylated RcsB can bind DNA as either a homodimer or a heterodimer with RcsA as a cofactor to either activate or repress DNA transcription [14]. Since deacetylation exposed a positive lysine residue in the DNA binding domain of RcsB which allowed it to bind DNA [14], then desuccinylation may serve the same purpose. Succinylated and desuccinylated lysine may be a stronger regulator for gene transcription since rather than a switch between neutral to positive, it is a switch between negative to a positive state. We investigated RcsB's DNA binding capabilities *in vitro* using CobB WT and R95M and found that desuccinylation increased DNA binding while deacetylation had no significant affect.

RESULTS/DISSUSSION

The CobB gene was amplified from *E. coli* K-12 by PCR and cloned into pET-28a expression vector using BamHI and XhoI restriction sites. The protein is then purified to near homogeneity by gravity flow chromatography using nickel affinity chromatography. Substrates were synthesized based on the H3K9 sequence with two Trp on the C-terminus to facilitate detection by ultra-violet (UV) light absorption. Activity was detected by analytical high pressure liquid chromatography (HPLC). Based on sequence alignment, CobB is also a type III sirtuin

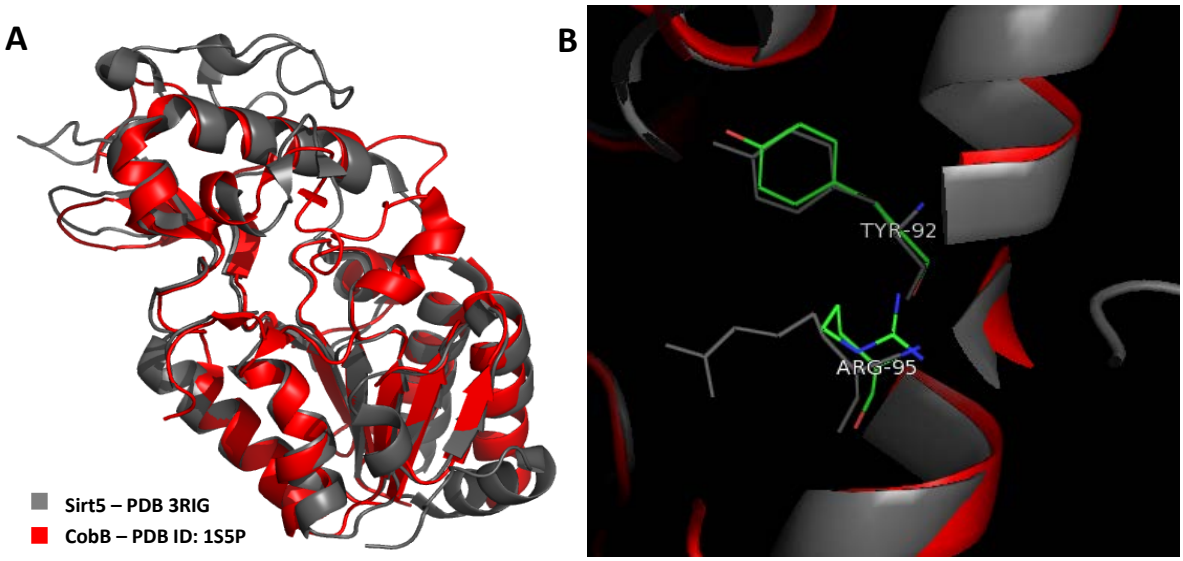

Figure 3. A) Alignment of Sirt5 (gray PDB 3RIG) and CobB (red PDB 1S5P). B) CobB's active site has two conserved residues, Tyr92 and Arg95, that are conserved in all type III sirtuins. The residues are important for desuccinylation activity of class three sirtuins. Pymol 1.3 was used to view the structures.

bearing the two conserved residues, Tyr92 and Arg95 (Fig. 3), which is suspected to be responsible for Sirt5's desuccinylation activity. Site-directed mutagenesis by PCR was used to make Y92F, R95M, and Y92F/R95M mutants which were subsequently cloned into pET-28a expression vector and purified the same way.

The acylated H3K9 peptides were used to investigate the activity of CobB and it's mutants and revealed that wildtype CobB has both deacetylase as well as desuccinylase activity while the active site mutants mainly retained their deacetylase activity. Kinetic studies were then carried out to quantitatively compare CobB's activity and assess the importance of the two active site residues for desuccinylation. The kinetics data in Table 2 suggests that wildtype CobB's deacetylase activity is 3 times stronger than it's desuccinylase activity, while R95M and Y92F/R95M mutants only has a k_{cat}/K_M of 22 sec^{-1} M^{-1} for succinylated H3K9 peptide, almost 100 fold lower when compared to wildtype CobB. The Y92F mutant's desuccinylase activity is 3 folds better than the other two mutants but is still considerably diminished when compared to wildtype CobB's original activity. All 3 mutants also suffered a 3 fold difference in terms of its deacetylation activity, retaining a similar K_M value but a lowered k_{cat} value. The desuccinylation values of the active site mutants were estimated based on a manipulation of the michaelis-menten equation.

Table 2 . Kinetics data of CobB and mutants with acetylated and succinylated H3K9 (KQTARK*STGGWW) peptides. Activity assay were done in duplicates and analyzed by analytical LC and curved was fitted with Kaleidograph v. 3.5.

		k_{cat} (sec^{-1})	K_M for Peptide(μM)	k_{cat} / K_M (sec^{-1} M^{-1})
H3K9 AC	**CobB WT**	0.135 ± 0.007	15.1 ± 0.424	9.0×10^3
	Y92F	0.052 ± 0.012	14.7 ± 2.26	3.5×10^3
	R95M	0.059 ± 0.002	20.0 ± 1.41	2.9×10^3
	Y92F/R95M	0.085 ± 0.037	29.3 ± 13.9	2.9×10^3
H3K9 SU	**CobB WT**	0.242 ± 0.040	86.3 ± 11.0	2.9×10^3
	Y92F	N/A	N/A	6.7×10^1
	R95M	N/A	N/A	2.2×10^1
	Y92F/R95M	N/A	N/A	2.2×10^1

The kinetic's study had revealed that both residues are critical for desuccinylation activity while having very little effect on deacetylation. This backs up the hypothesis that all type III sirtuins that have a conserved Tyr and Arg residue in its activity site should be a desuccucinylase.

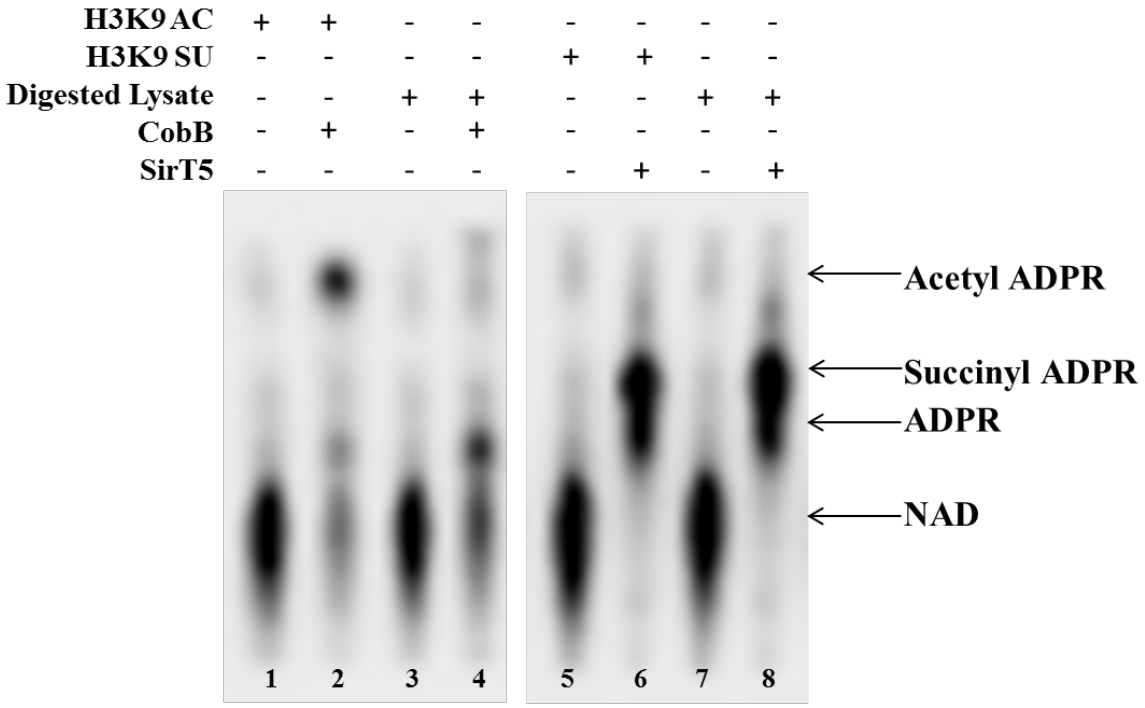

Figure 4. ^{32}P-NAD activity assay of trypsin digested *E. coli* total cell lysate. The peptide solution is then treated with either CobB or sirt5 and the resulting acylated ADPR is separated on a TLC. Lane 1 and 5 is acetylated or succinylated H3K9 peptide only, lane 2 and 6 is either CobB or Sirt5 with acetylated or succinylated H3K9 peptide. Lane 3 and 7 is digested lysate only and lane 4 and 8 is the digested lysate with CobB and Sirt5. Acetylated and succinylated ADPR is detectable in the digested cell lysate in lanes 4 and 8 suggesting that acetylated and succinylated proteins are present in *E. coli*.

To investigate the physiological importance of desuccinylation, *E. coli* cell lysates were trypsin digested and the peptides were investigated for the presence of lysine succinylation. To investigate we used ^{32}P-NAD activity assay, a mechanism based method in which NAD molecules with a radiolabeled phosphorus will be consumed by sirtuins to generate radiolabeled acylated ADPR, to investigate. In Figure 4, digested cell lysates were treated with either CobB or Sirt5 and succinylated ADPR was generated and detected by thin layer chromatography

(TLC). The promiscuity of CobB's activity makes it difficult to generate a clean acylated ADPR spot, hence Sirt5 is used to better detect desuccinylation.

Many approaches were used to find a succinylated substrate for CobB. A literature search revealed several acetylated CobB substrates and those were investigated first since in the case of Sirt5, CPS1 demonstrated that it can both be a lysine deacetylation and desuccinylation target [16]. We had also hypothesized that CobB was important for metabolism since that is the main function of CobB in *S. enterica*. Acetyl-CoA synthetase (ACS) plays a crucial role in the TCA cycle and can be activated by the deacetylation of a lysine residue [11]. We identified several metabolic *E. coli* proteins that were succinylated including 2-oxoglutarate dehydrogenase, E1 component (SucA), Serine hydroxymethyltransferase (GlyA), Histidine protein kinase sensor of chemotactic response (CheA), and isocitrate dehydrogenase (ICD) by ^{32}P-NAD activity assay (Fig. 5A-C). These proteins suggested that succinylation and hence CobB may be involved in metabolism since it is the only known desuccinylase in *E. coli.*

Literature had suggested that different feeding conditions will affect the acetylation levels in the cell [22]. We investigated the importance of CobB under several different metabolic conditions by varying the carbon source. A CobB KO strain was grown in minimal media with either acetate, succinate or propionate as the sole carbon source and the observed phenotype was compared to its parent strain. Originally it was thought that succinate supplemented cells would have the greatest observable phenotype but experimentally acetate and propionate supplemented cells demonstrated the greatest growth difference (Fig. 6). The phenotypes demonstrated by the growth curves in Figure 4 can be attributed to either CobB's deacetylation or desuccinylation function. To further investigate the individual functions of CobB, we transformed back either the CobB or R95M gene in the KO strain and repeated the

growth experiment. In Figure 5, transforming back either the CobB or R95M gene only demonstrated an effect in acetate and propionate supplemented cells. In acetate supplemented cells, it seems that desuccinylation may actually be detrimental to acetate metabolism. Although propionate supplemented cells demonstrated the greatest difference between CobB parent and CobB KO strain, it can be concluded that the detriment in growth is most likely the result of deacetylation [23]. Cells transformed with either CobB or R95M had similar growth profiles and had a shorter lag phase than cells transformed back with H147Y, a catalytic mutant of CobB with no activity.

CobB's function in *E. coli* has not been well studied, but two deacetylation substrates were identified, CheY and RcsB [14, 24]. Deacetylation of CheY affects chemotaxis while deacetylation of RcsB is important in gene regulation [14, 24]. Other possible substrates were identified through proteonomic studies by the Zhao group [25]. Succinylated proteins are not necessary substrates of CobB since chemical succinylation is a possibility with succinyl-CoA as the donor [26-29].

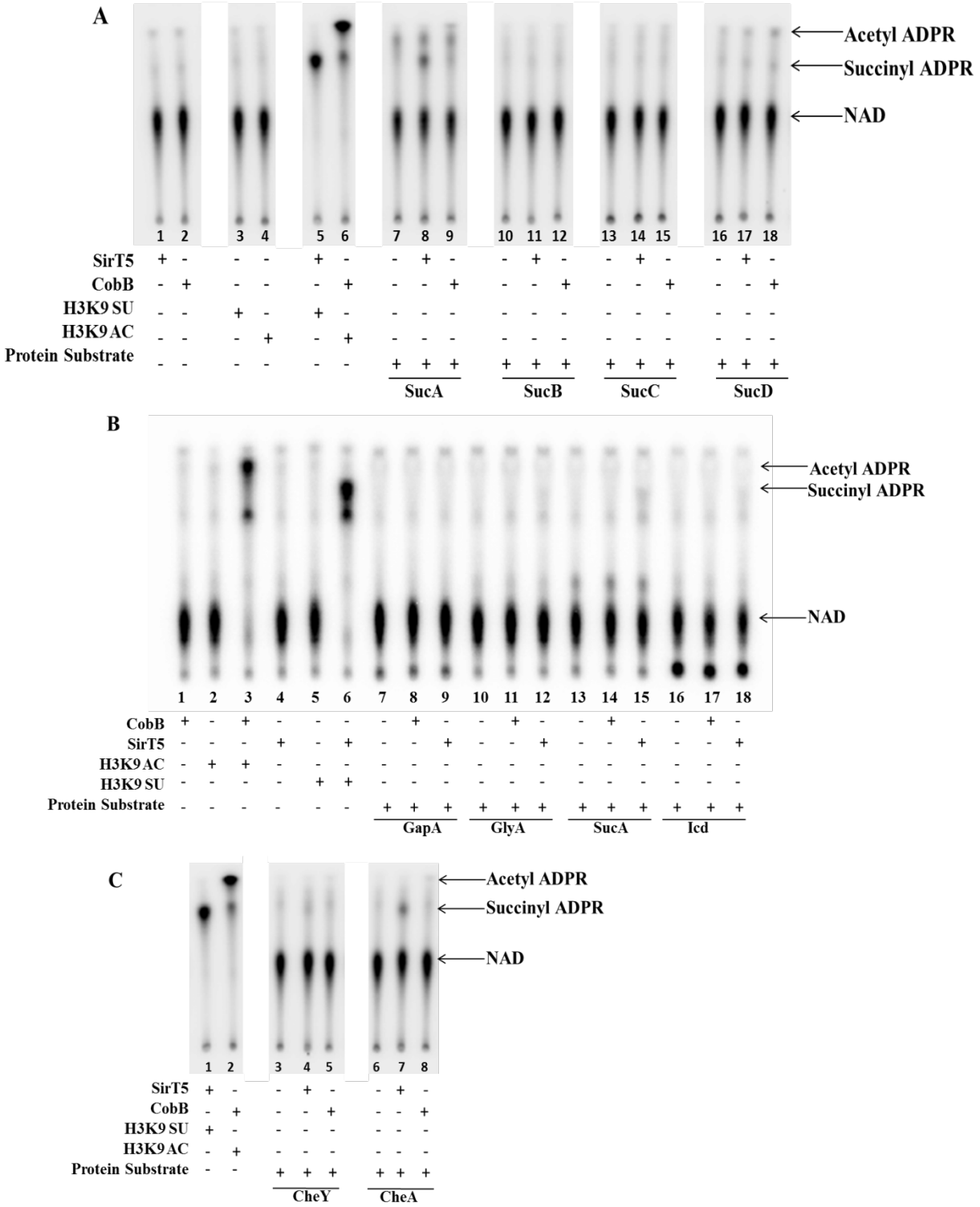

Figure 5. ^{32}P-NAD activity assay of possible CobB substrates. Proteins were expressed in LB media and NiNTA purified. A) SucA-SucD forms a protein complex that is essential for metabolism. SucA is observed with the strongest succinyl spot in lane 8, which is treated by Sirt5. In lane 9, SucA is treated with CobB and the acylated ADPR smear suggests that SucA may have other PTM's aside from acetyl and succinyl. B) Substrates identified by the Zhao lab to be potential CobB targets for desuccinylation. Only GlyA and ICD have observable succinyl ADPR spots. C) CheY was identified as a CobB deactylation target responsible for a role in chemotaxis however, interestingly enough, CheA was identified with a stronger succinyl ADPR spot while CheY had no detectable acetyl or succinyl ADPR.

A)

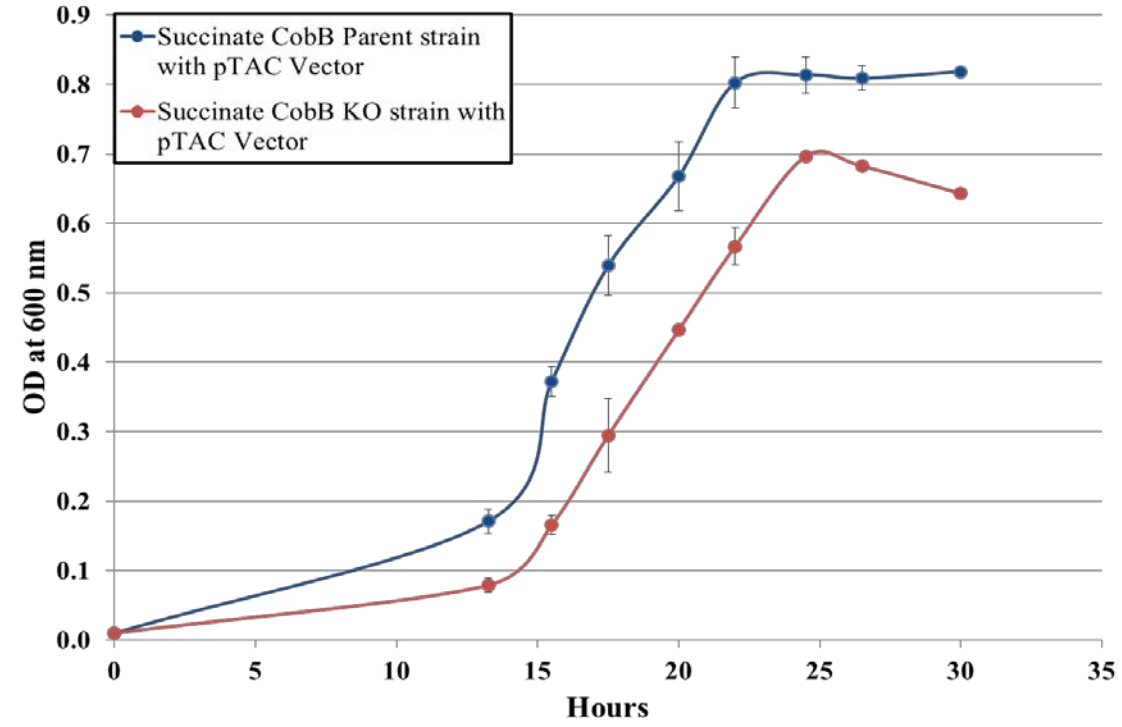
Growth Comparison of CobB Parent and KO Strain in Minimal Media with Succinate as Sole Carbon Source
Succinate CobB Parent strain with pTAC Vector
Succinate CobB KO strain with pTAC Vector
OD at 600 nm
0.0
0.1
0.2
0.3
0.4
0.5
0.6
0.7
0.8
0.9
0
5
10
15
20
25
30
35
Hours

B)

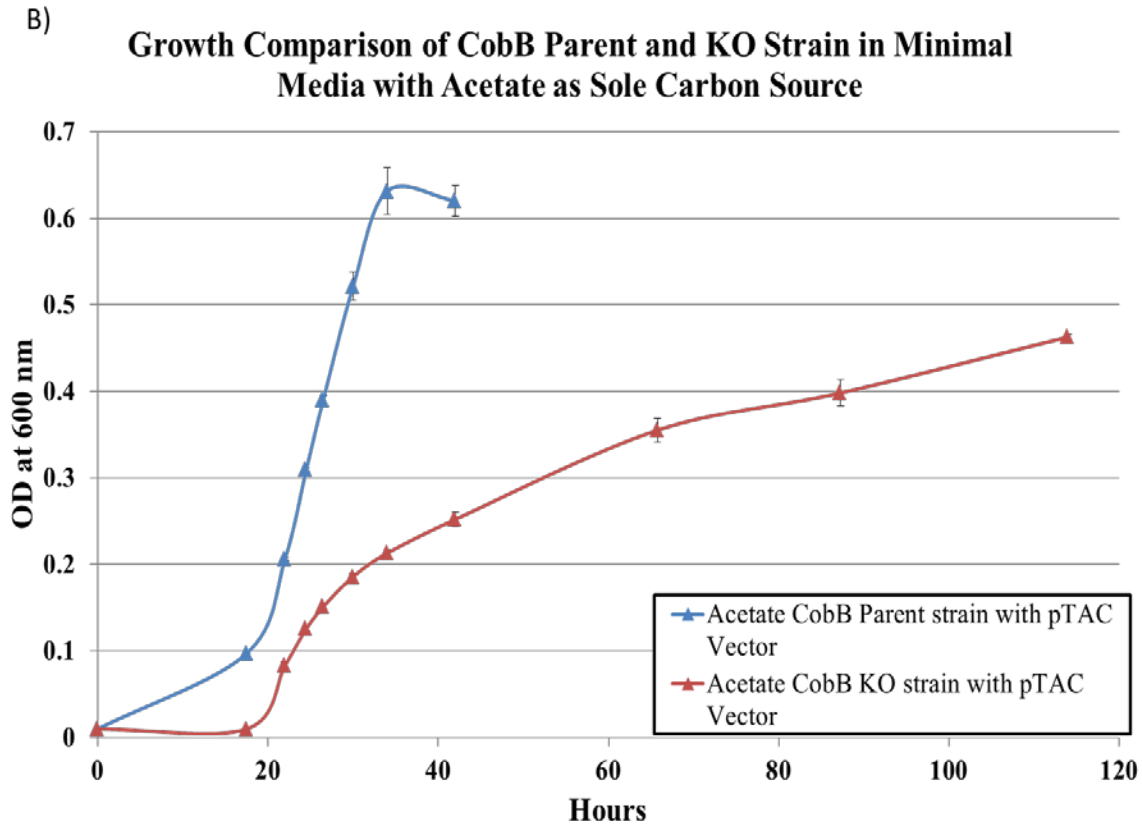
Growth Comparison of CobB Parent and KO Strain in Minimal Media with Acetate as Sole Carbon Source
Acetate CobB Parent strain with pTAC Vector
Acetate CobB KO strain with pTAC Vector
OD at 600 nm
0
0.1
0.2
0.3
0.4
0.5
0.6
0.7
0
20
40
60
80
100
120
Hours

C)

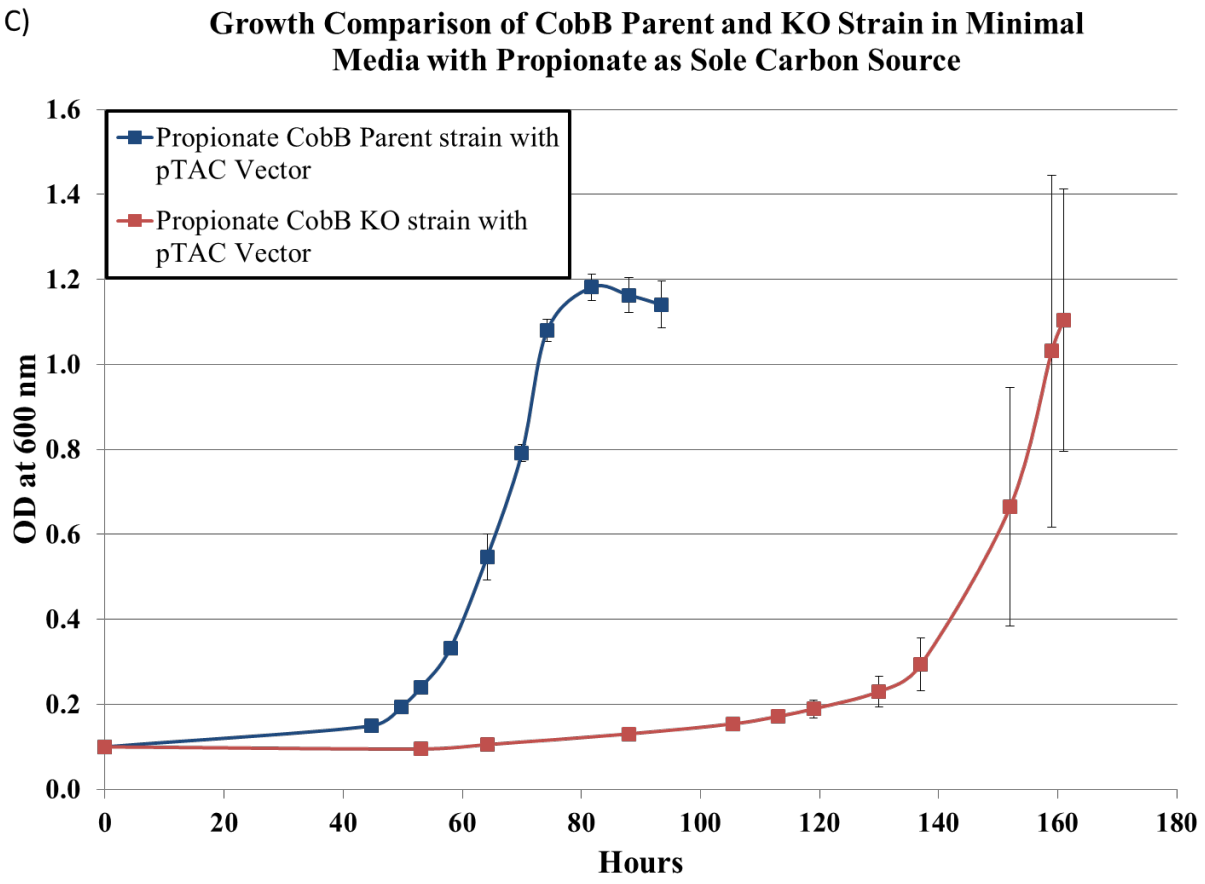

Figure 6. Growth Comparison of CobB parent and KO strain grown in minimal media with succintate, acetate, or propionate as a carbon source. Blue lines represent the CobB parent strain and the red line represents CobB KO strain. The circle represents media supplementation with succinate, the triangle represents media supplementation with acetate and the square represents media supplementation with propionate. The error bars are derived from two trials. All the strains observed a lag phase when grown in media with unconventional carbon source. Succinate only had the shortest lag before the exponential phase while acetate and propionate had a lag phase of about 20 hours for acetate and over 40 hours for propionate supplemented cells. While acetate and succinate had similar lag phases, propionate demonstrated the largest phenotype for growth. The parent CobB strain only had a lag phase of over 40 hours while the KO CobB strain nearly tripled that time. Interestingly, there is no great difference in terms of the doubling time during exponential phase or a difference in final OD. The succinate supplemented cells had only final OD differences similar to that of acetate grown cells, but unlike the acetate cells, whose doubling time of the KO strain was significantly different than that of the wildtype, the succinate doubling time remains the same between both strains.

A)

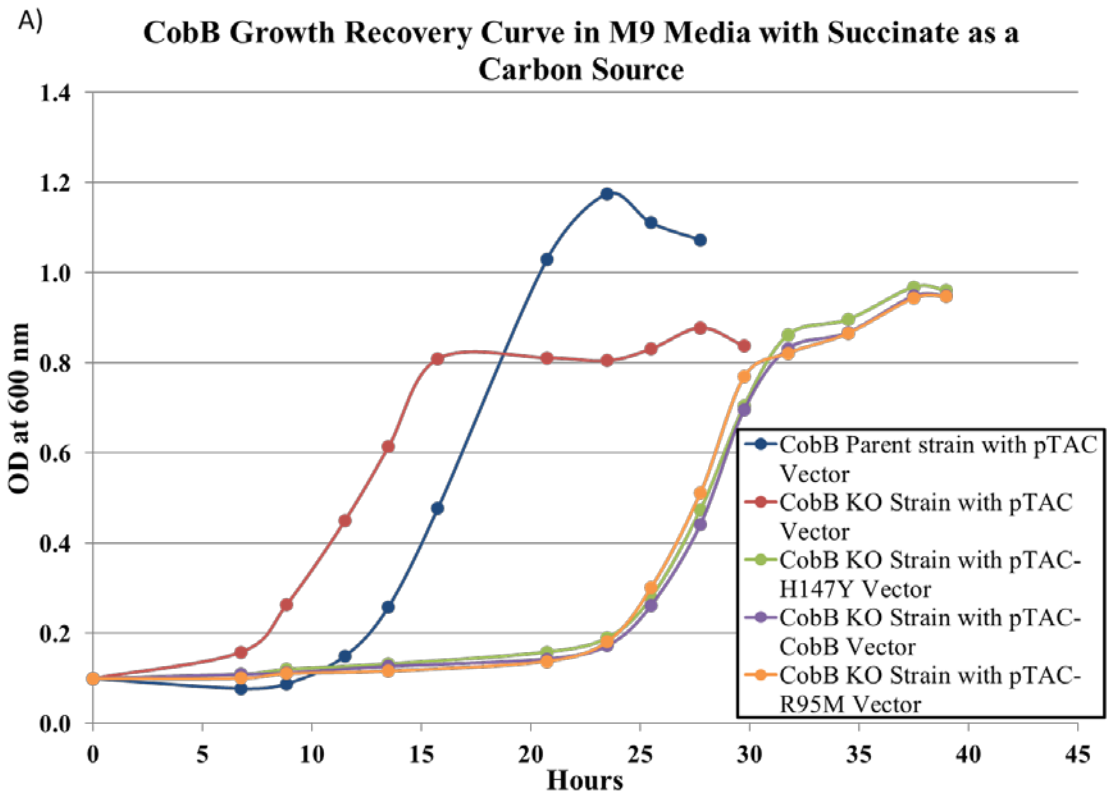
CobB Growth Recovery Curve in M9 Media with Succinate as a Carbon Source
OD at 600 nm
Hours
CobB Parent strain with pTAC Vector
CobB KO Strain with pTAC Vector
CobB KO Strain with pTAC-H147Y Vector
CobB KO Strain with pTAC-CobB Vector
CobB KO Strain with pTAC-R95M Vector

B)

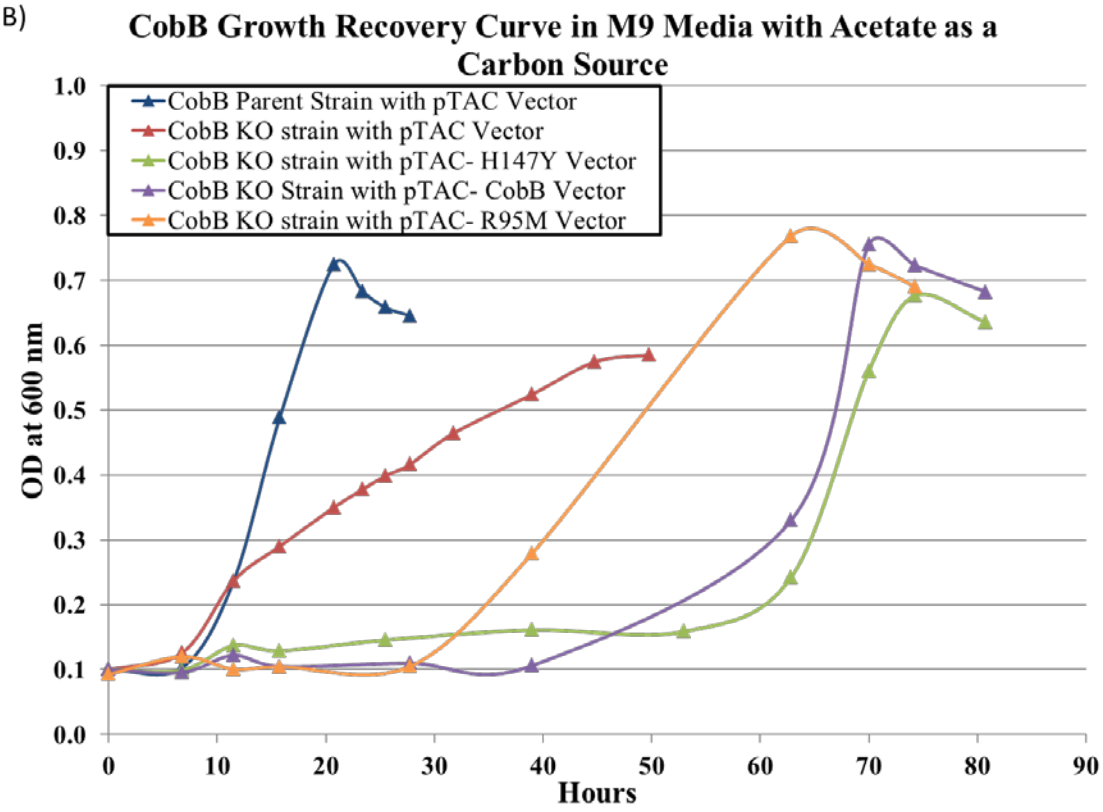
CobB Growth Recovery Curve in M9 Media with Acetate as a Carbon Source
OD at 600 nm
Hours
CobB Parent Strain with pTAC Vector
CobB KO strain with pTAC Vector
CobB KO strain with pTAC- H147Y Vector
CobB KO Strain with pTAC- CobB Vector
CobB KO strain with pTAC- R95M Vector

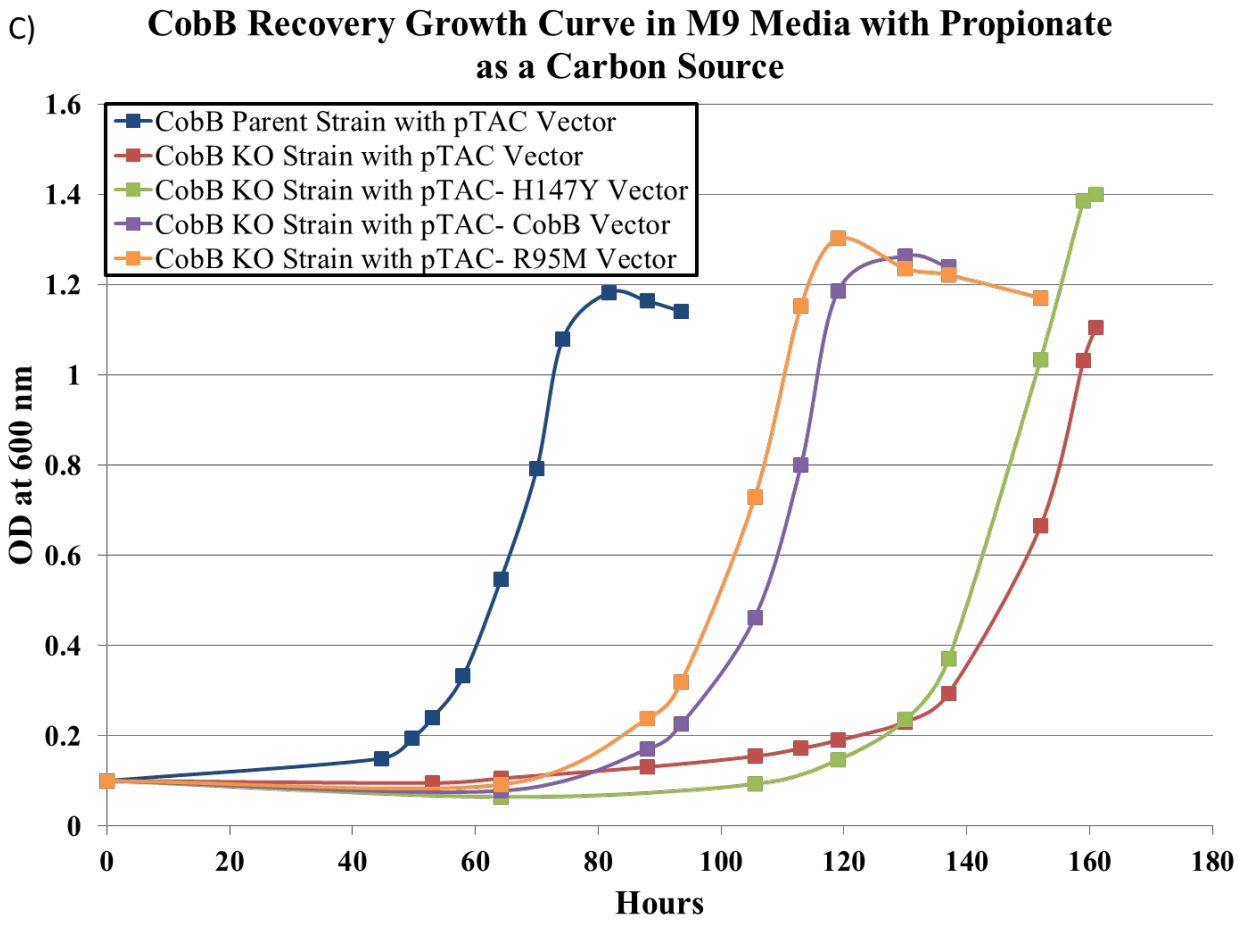

Figure 7. CobB recovery growth curve. The circle represents media supplementation with succinate, the triangle represents media supplementation with acetate and the square represents media supplementation with propionate. Blue represents the CobB parent strain with the empty pTAC vector. Red represents the CobB KO strain with the empty pTAC vector. Green represents the CobB KO strain with H147Y transformed back. Purple is CobB KO strain with WT CobB transformed back. Orange is CobB KO strain with R95M transformed in. The H147Y is a catalytic mutant of CobB with activity and it serves as a control to eliminate protein association effect of CobB expression. In acetate supplemented media it appears that R95M may be most beneficial to the KO strain implying that desuccinylation is detrimental to acetate metabolism. In succinate supplemented cells CobB does not appear to have any affect in the succinate metabolism, while in propionate supplemented cells, the improvement in phenotype may most likely be attributed to deacetylation function of CobB since R95M and WT CobB had a similar growth curve.

Suspected substrates were expressed and NiNTA purified from ASKA (-) strains which bears an N-terminal hexahistidine tag. The purified proteins were then investigated using the above mentioned ^{32}P-NAD activity assay. Only one protein, RcsB, had showed promising results after CobB treatment. RcsB is regulated by PAT and CobB and when it is deacetylated on Lys180, it can bind DNA and hence regulate gene expression. A DNA shift assay in Figure 8 shows that when RcsB was pretreated with CobB prior to the addition of DNA, it can bind more DNA than the untreated RcsB. What was more interesting was when RcsB was treated with R95M, which has deficient desuccinylase activity, it exhibited similar amount of DNA binding to the untreated RcsB protein. This suggests that desuccinylation may be responsible for the increased ability of RcsB to bind DNA. Since R95M has a weaker *in vitro* deacetylation activity than CobB, the difference in DNA binding may still be a result of deacetylation. zWe investigated CobB and R95M's ability to deacetylate and desuccinylate RcsB by pretreating RcsB with untagged CobB and R95M. RcsB was NiNTA purified and eluted with 250 mM of imidazole. Buffer exchange columns were then used to eliminate NAD and to concentrate RcsB. In Figure 9, the pretreated RcsB's were then treated again with CobB or Sirt5 in the ^{32}P-NAD activity assay and TLC was used to separate acetyl and succinyl ADPR. The data suggests that CobB can remove more succinyl but less acetyl groups from lysine residues than R95M treated RcsB. This evidence in conjunction with the DNA shift assay strongly suggests that RcsB is regulated by desuccinylation rather than by deacetylation.

In summary, we can conclude that the Arg and Tyr residues are essential to desuccinylation of type III sirtuins. We have demonstrated with our enzymology data that CobB can deacetylate and desuccinylate efficiently with only a 3 fold difference.

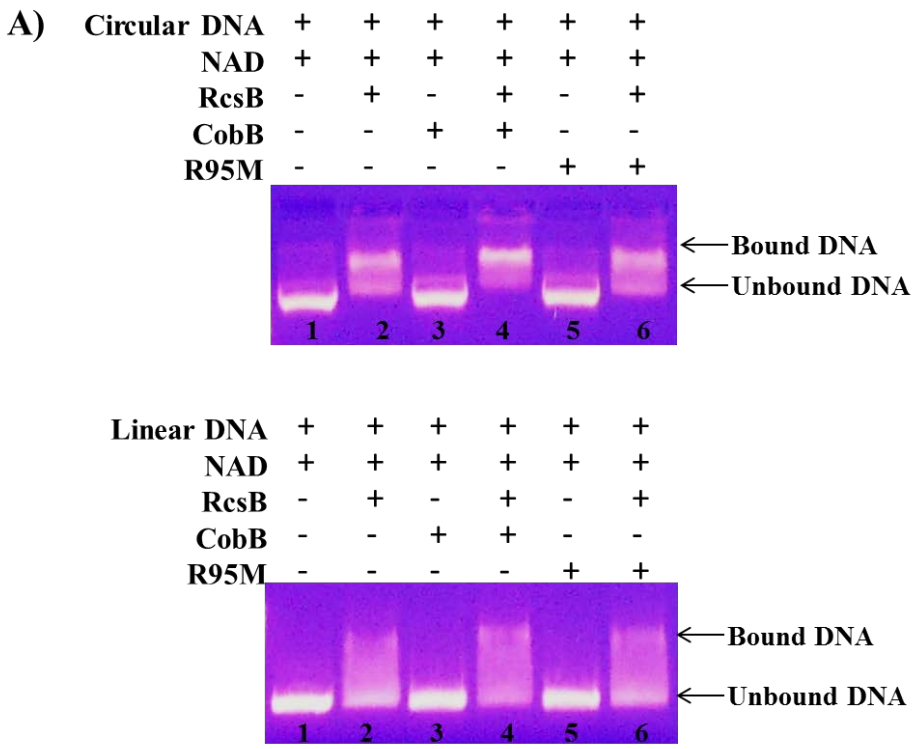

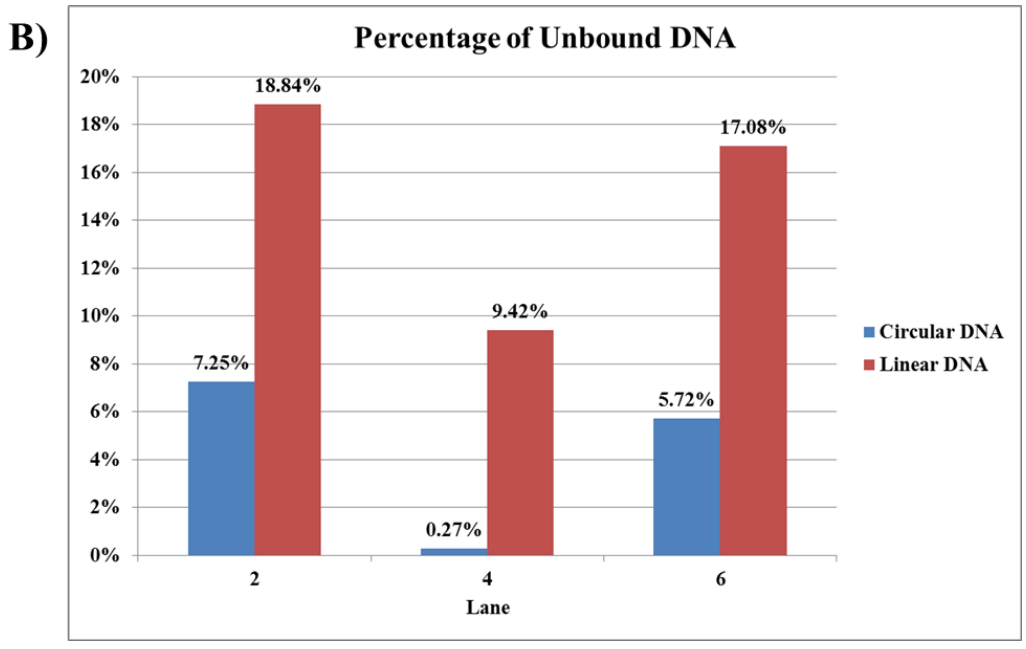

Figure 8. A) DNA shift assay. RcsB is pretreated with CobB or R95M and then incubated with either circular or linear DNA. There is a noticeable increase in band intensity in lane 4,where CobB treated RcsB allows it to bind more DNA. The Untreated and R95M treated RcsB has similar band intensities for bound DNA suggesting that CobB's dessucinylation activity may be responsible for regulating RcsB rather than deacetylation. B) Percentage of unbound DNA calculated using ImageJ.

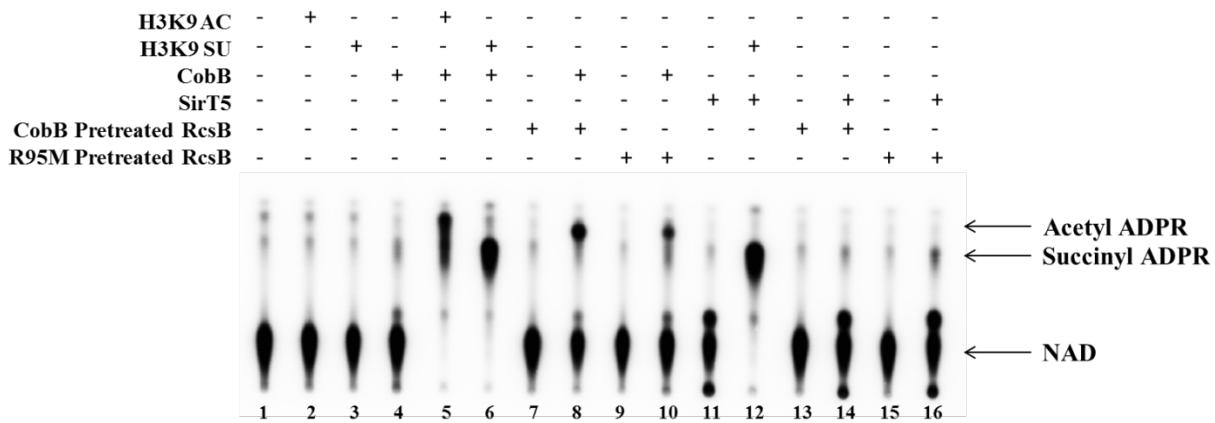

Figure 9. TLC of ^{32}P-NAD activity assay of CobB and R95M treated RcsB. The enzyme treated RcsB is treated with either CobB, for the detection of both succinyl and acetyl levels, or Sirt5, for the detection of succinyl levels on RcsB. Lane 8 and lane 9 indicates that CobB treated RcsB has a weaker succinyl ADPR spot than and a stronger acetyl ADPR spot than RcsB treated by R95M. Lane 13 and lane 16 is consistent with what was observed in lane 8 and 9. The data suggests that CobB can remove more succinyl groups off of RcsB while R95M can remove more acetyl groups.

Growth comparison between CobB and CobB KO strain under different nutrient conditions, suggests that CobB is most likely involved in many metabolic pathways. CobB had the strongest effect in propionate supplemented media but recovery experiments with mutant CobB, R95M, to WT CobB, suggesting that depropionylation of propionyl-CoA synthetase (PrpE) is likely the cause of the lag phase difference [23]. Propionyl is very similar to acetyl. Even though we do not have kinetics with H3K9 Propionyl, we can hypothesize that it would be very similar to H3K9 AC data. Although it appears that CobB is important in some metabolic pathways, the effect of it's desuccinylase activity in metabolic regulation is unclear. However, in terms of gene regulation, we provided strong evidence to support that RcsB is regulated by CobB through desuccinylase activity rather than deacetylase activity. More work is needed in the identification of succinyltransferases, to demonstrate that, like lysine acetylation, lysine succinylation is also a reversible reaction used to regulate gene transcription.

METHODS

Cloning, expression, and purification of CobB amd Mutants. CobB gene was PCR amplified from *E.coli* K-12 and cloned into pET-28a(+) vector with BamHI and XhoI restriction sites. The CobB expression vector was then introduced into an *E. coli* BL21 with pRARE2. Successful transformants were selected by plating the cells on kanamycin (50 mg mL^{-1}) and chloramphenicol (20 mg mL^{-1}) luria broth (LB) plates. Single colonies were selected and grown in LB with kanamycin (50 mg mL^{-1}) and chloramphenicol (20 mg mL^{-1}) overnight at 37^{o}C. On the following day the cells were then subcultured (1:1000 (v/v)) into a 2 L LB with kanamycin (50 mg mL^{-1}) and chloramphenicol (20 mg mL^{-1}). The cells were induced with 500 μM of isopropyl β-D-1-thiogalactopyranoside (IPTG) at OD_{600} of 0.6 and grown overnight at 15^{o}C, 200 rpm. The cells were harvested by centrifugation at 6000 rpm for 10 minutes at 4^{o}C (Beckman Coulter Refrigerated Floor Centrifuge) and passed through an EmulsiFlex-C3 cell disruptor (AVESTIN, Inc.) 3 times. Cellular debris was removed by centrifuging at 20000 rpm for 30 minutes at 4^{o}C (Beckman Coulter). The CobB was then purified using gravity flow Ni-affinity chromatography (Sigma) and dialyzed into 25 mM Tris pH 8.0, 150 mM NaCl, 1 mM DTT, 10% (v/v) glycerol. The proteins were then aliquoted and kept frozen at -80^{o}C. The active site and catalytic mutant of CobB, Y92F, R95M, Y92F?R92M and H147Y, were made by PCR site directed mutagenesis and expressed and purified the same way as wildtype CobB.

Synthesis of acyl peptides. Solvents were purchased from Fisher Scientific unless otherwise specified and peptide synthesis reagents and Fmoc-protected amino acids and derivatives were purchased from Creosalus Inc.

The H3K9 (NH_2-KQTARK*STGGWW-COOH) backbone was prepared using standard solid phase peptide synthesis (SPPS) at room temperature (RT). Wang resins SS (100-200 mesh,

1% DVB, 10 mmole/g) were placed into a peptide synthesis vessel along with 5 mL of anhydrous dichloromethane (DCM) for 5 hours. The first activated amino acid solution was freshly prepared with 0.32 mmoles of Fmoc-W-OH, 0.32 mmoles of O-benzotriazole-*N*,*N*,*N'*,*N'*-tetramethyl-uronium-hexafluoro-phosphate (HBTU), 0.133 mmoles of 4-dimethylaminopyridine (DMAP), 0.64 mmoles of diisopropylethylamine (DIEA, added last) and an appropriate amount of anhydrous *N*,*N'*-dimethylformamide (DMF). The resin was incubated with the solution overnight at RT. The resins were then washed with DMF (5 times) before incubating with a cocktail of acetic anhydride, pyridine and DMF (2:1:3 ratio (v/v)) for 30 minutes to block remaining amino groups on the resin. Kaiser test was used to test the success of the coupling. Once coupling was confirmed, 20% (v/v) piperidine in DMF was used to remove Fmoc. All subsequent activated amino acid derivatives were freshly prepared with 0.24 mmoles of the amino acid, 0.24 mmole of HBTU, 0.21 mmole of N-hydroxybenzotriazole (HOBT), 0.48 mmole of DIEA in DMF and reaction time was 2 hours at RT.

The lysine to be modified by different acyl groups (K*) was protected with allyl carbamate (Alloc) on the side chain while the N-terminal K was protected by Boc. After all the peptide coupling steps were done on the resin, the Alloc group was removed by incubating the resin in a cocktail of DCM, morpholine (Sigma, 2.5%) and glacial acetic acid (5%) with a 1:1 weight ratio of the original resin and tetrakis(triphenylphosphine)palladium(0) for 4 hours under nitrogen. Several washes of 0.5% (v/v) DIEA in DCM and 0.02 M of diethyldicarbamate in DMF were carried out to remove the palladium. The resin was then incubated with solutions for putting on different acyl groups. The acylation solutions contained 0.24 mmoles of the different groups (acetic anhydride, succinic anhydride), 0.24 mmole of HBTU, 0.21 mmole of HOBT, 0.48 mmole of DIEA and DMF. The resin was then washed with DMF and the peptides were cleaved

with a mixture of trifluoroacetic acid (TFA), 5% (v/v) water, 5% (w/v) phenol, 2.5% (v/v) ethanedithiol and 5% (v/v) thioanisole. TFA was removed from the filtered peptide solution and the peptides were precipitated out by the addition of ether and lyophilized. The crude peptides were dissolved in water and purified by HPLC (Beckman Coulter System Gold 125P solvent module and 168 Detector) using a TARGA C18 column (250 x 20 mm, 10 μM, Higgins Analytical, Inc.) with mobile phase A (water with 0.1% (v/v) TFA) and B (acetonitrile with 0.1% (v/v) TFA) at a gradient of 20% B to 100% B in 50 minutes and a flow rate of 10 mL/min. The peptides were monitored at 215 nm and 280 nm and fractions were collected. LCMS (SHIMADZU LCMS-QP8000α with a Sprite TARGA C18 column (40 × 2.1 mm, 5 μm, Higgins Analytical, Inc.) was used to confirm the peptide mass and high purity fractions were lyophilized. The solvents used in LCMS were water with 0.1% (v/v) formic acid and acetonitrile with 0.1% (v/v) formic acid.

HPLC assay and kinetics. Activity of CobB was determined using HPLC, by quantifying the modified and unmodified H3K9 peptide. The reaction contained 20 mM of Tris pH 8.0, 1 mM DTT, 20 μM H3K9 modified peptide, 1 mM of NAD and 0.5 μM of CobB and was incubated at 37^{o}C for 1 hour. The reaction was quenched with 1 volume of 10% (v/v) TFA and spun down for 10 minutes at 18,000 g (Beckman Coulter Microfuge) to separate the enzyme from the reaction. The supernatant was then analyzed by HPLC.

The k_{cat} and K_m values were determined using HPLC to quantify the amount of product formed with varying concentrations of the modified peptide with 1 mM of NAD, 20 mM Tris pH 8.0, 100 mM NaCl, 1 mM DTT, 0.5 μM of CobB (acetyl and succinyl H3K9 peptide). Peptide concentration used for H3K9 acetyl was 5, 8, 10, 12, 16, 32, 40, 67 and 268 μM and Succinyl

was 2, 3, 4, 6, 8, 12, 16, 24, 32 and 128 μM with an incubation time of 1 and 2 minutes, respectively for wildtype CobB and 3 mins for deacetylation for the mutants. Peptide concentration used for desuccinylation activity estimation of CobB mutants was 256 μM for 60 mins at 37^{o}C. The quenched reactions were then analyzed via HPLC using a reverse phase analytical column (Kinetex XB-C18 100A, 75x 4.60 mm, 2.6 um, Phenomenex) with a 0% to 70% B gradient in 20 minutes at 0.5 mL/min. The acetyl and succinyl peptide has a very close retention time to the unmodified peptide. The product peak and the substrate peaks were both quantified and converted to initial rates, which were then plotted against the modified peptide concentration and fitted using the Kaleidagraph program.

^{32}P-NAD activity assay. The reaction contained 50 mM Tris pH 8.0, 150 mM NaCl, 10 mM DTT, 60 μM H3K9 modified peptide, 0.1 μCi of ^{32}P-NAD (American Radiolabeled Chemicals, ARP 0141-250 μCi) and 1 μM of CobB or SirT5, and was incubated at 37^{o}C for 1 hour.

E. coli whole cell lysate (100 μL) was first denatured with 6 M of Urea, 15 mM of DTT at 37^{o}C for 1 hour. Then it was alkylated with 50 mM of iodoacetamide in the dark at RT for 1 hour. The solution was then diluted so that the final concentration of urea was less than 0.75 M and digested with 0.1 μg/μL trypsin and 50 mM Tris pH 7.4, and 1 mM $CaCl_2$ overnight at 37^{o}C. The digest was quenched with 10% (v/v) TFA to a final pH of 2 to 3 and desalted with a Waters C18 Sep-Pak column. The peptides were eluted 5 times with 1 mL of 50% (v/v) ACN/0.1% (v/v) TFA and lyophilized. The peptides were then solubilized in 50 μL of water and 1 μL was used in the ^{32}P-NAD assay under conditions described above. The reaction was incubated at 37^{o}C for 1 hour and 0.5 μL of the reaction mixture was spotted onto a polyester backed silica

plate (100 µm thick, Waters). After the spots were dried, the plate was run for 6 cm in 30:70 (v/v) 1M ammonium bicarbonate: 95% ethanol. The plate was dried and exposed overnight in a PhosphorImaging screen (GE Healthcare). The signal was detected using a STORM860 phosphorimager (GE Healthcare).

Growth curve. Chemically competent CobB parent and KO *E. coli* cells, transformed with either empty pTAC vector or pTAC-H147Y, pTAC-CobB, pTAC-R95M plasmids, are grown in a LB starter culture with 100 mg mL^{-1} of ampicillin at 37^{o}C for 24 hours. The starter culture is then spun down at 4000 rpm and 4^{o}C for 15 mins and washed twice with minimal media. The cells are resuspended again in minimal media with no supplements and placed in a shaker incubator for 2 hours at 37^{o}C and 200 rpm. This step serves to deplete the cell of LB nutrients that will interfere with the growth curve later on. After the 2 hour, cells are normalized to an OD_{600nm} of 1.0 and subcultured into minimal media with 2 mM $MgSO_4$, 0.1 mM $CaCl_2$, 34 µg $µL^{-1}$ of thiamine, 0.003% of $FeSO_4$, 100 mg mL^{-1}Ampicillin, 1 mM IPTG, and either 20 mM of sodium acetate, 16.5 mM of sodium succinate or 22 mM of sodium propionate with a starting OD_{600nm} of either 0.01, 0.05 or 0.1. The OD_{600nm} of cells are monitored every 2 hour intervals for succinate, 4-8 hour intervals for acetate and 6-12 hour intervals for propionate supplemented cells. Ampicillin and IPTG are replenished every 48 hours to enable selection pressure for the pTAC plasmid. When cells reach the stationary phase they are spun down at 4000 rpm for 15 mins at 4^{o}C and stored for PCR analysis. Using sequencing primers, N26 and C24, for the pTAC plasmid we use PCR to ensure that the cells still have the plasmid during the long period of growth.

DNA shift assay. NiNTA purified RcsB (final 2.5 µM) is incubated with 2.5 µM final concentration of CobB or R95M for 1 hour at 37^{o}C in 25 mM of sodium phosphate buffer pH

8.0, 100 mM of NaCl, and 1 mM of NAD. After the hour, 5 µg μL^{-1} of pTAC plasmid or 20 µg μL^{-1} of an 800 bp PCR fragment is added and the mixture is incubated at room temperature for 1 hour before the reaction is quenched with 5 µL of DNA dye. The reaction is loaded onto a 0.7% DNA gel with ethidium bromide and run at 150 V for 40 mins. The result is visualized by a UV light box and picture is taken by a canon camera.

CobB and R95M pretreatment of RcsB. Histag pTEV was incubated with CobB or R95M at 30^{o}C for 1 hour in 25 mM of TRIS pH 8.0, 100 mM NaCl and 1 mM of DTT. The mixture is then incubated with 100 uL of NiNTA (Qiagen) resin for an hour at 4^{o}C to remove all histag proteins leaving just untagged protein. The mixture is loaded onto a 1.5 mL spin column and the resin was separated from the mixture. Then the untagged proteins were incubated with histagged RcsB at a ratio of 1:10 and 1 mM NAD for an hour at 37^{o}C. After the hour 100 uL of NiNTA (Qiagen) was incubated with the mixture for 1 hour at 4^{o}C and loaded onto a spin column. The resin is then washed twice with 10 mM imidazole and RcsB is eluted with 250 mM of imidazole. The elution is then loaded onto a0.5 mL buffer exchange column (Millipore) to remove NAD and concentrate the sample. Final buffer content is 25 mM TRIS pH 8.0, and100 mM NaCl. The CobB and R95M treated protein concentration is normalized to 24 µM and used in a ^{32}P-NAD activity assay with 2.5 µM final concentration of either CobB or SirT5 for 1 hour at 37^{o}C. The rest is the same as ^{32}P-NAD activity assay mentioned about.

CHAPTER 3: *PLASMODIUM FALCIPARUM* SIR2A PREFERENTIALLY HYDROLYZES MEDIUM AND LONG CHAIN FATTY ACYL LYSINE

ABSTRACT

Plasmodium falciparum Sir2A (PfSir2A), a member of the sirtuin family of nicotinamide adenine dinucleotide-dependent deacetylases, has been shown to regulate the expression of surface antigens to evade the detection by host immune surveillance. It is thought that PfSir2A achieves this by deacetylating histones. However, the deacetylase activity of PfSir2A is weak. Here we present enzymology and structural evidences supporting that PfSir2A catalyzes the hydrolysis of medium and long chain fatty acyl groups from lysine residues more efficiently. Furthermore, P. falciparum proteins are found to contain such fatty acyl lysine modifications that can be removed by purified PfSir2A in vitro. Together, the data suggest that the physiological function of PfSir2A in antigen variation may be achieved by removing medium and long chain fatty acyl groups from protein lysine residues. The robust activity of PfSir2A would also facilitate the development of PfSir2A inhibitors, which may have therapeutic value in malaria treatment.

Published in ACS Chem Bio.

Accession number 21992006

Sirtuins are a family of enzymes known as nicotinamide adenine dinucleotide (NAD)-dependent deacetylases [30, 31]. They regulate a variety of biological processes, including transcription and metabolism [32, 33]. *Plasmodium falciparum* (*P. falciparum*) contains two sirtuins, PfSir2A and PfSir2B [34]. It was shown that these two sirtuins regulate the expression of surface antigens to evade the detection by host immune surveillance [35, 36]. Thus, inhibiting these sirtuins may help fight malaria. It was thought that PfSir2A and PfSir2B achieve this physiological function by deacetylating histones. *In vitro* studies on PfSir2A showed that it has deacetylase activity [37]. However, the activity was weak compared to several other sirtuins [38], such as human Sirt1 and yeast Sir2. It was also reported that PfSir2A had ADP-ribosyltransferase activity [37]. However, several reports questioned whether the ADP-ribosyltransferase activity of sirtuins was physiologically relevant since the measured activity of several sirtuins was weak [39, 40].

In addition to acetylation, lysine propionylation and butyrylation have been reported as posttranslational modifications that occur on proteins, including histones [23, 41, 42]. Many fatty acyl-CoA molecules exist in cells as metabolic intermediates. If the shorter chain fatty acyl CoA molecules (acetyl-CoA, propionyl-CoA, and butyryl-CoA) are used as acyl donors to modify proteins, it is possible that longer chain fatty acyl-CoA molecules can also be used to modify protein. Given that PfSir2A's deacetylase activity is weak, we set out to investigate whether longer chain fatty acyl lysine can be accepted as better substrates by PfSir2A.

The PfSir2A gene was de novo synthesized. The protein was expressed in *E. coli* and affinity purified to near homogeneity. For substrates, we synthesized histone H3 peptides bearing acetyl, butyryl, octanoyl, and myristoyl groups on Lys9. To facilitate the detection of the peptides by ultra-violet (UV) light absorption, two Trp residues were added to the C-terminal of

the peptides. A high-pressure liquid chromatography (HPLC) assay was used to monitor the activity of PfSir2A on these different acyl peptides. Interestingly, all four acyl peptides could be hydrolyzed (Fig. 10a). The butyryl, octanoyl and myristoyl peptides could be hydrolyzed more efficiently than the acetyl peptide. The myristoyl peptides appeared to be hydrolyzed most efficiently.

To quantitatively compare the activity of PfSir2A on different acyl peptides, kinetic studies were carried out. The kinetics data (Table 3) suggested that acetyl H3K9 peptide was the least efficient substrate among the four acyl peptides tested, with a k_{cat}/K_m of 26 $s^{-1}M^{-1}$. The k_{cat}/K_m value for deacetylation was comparable to that reported by Sauve and coworkers [38]. The butyryl, octanoyl, and myristoyl peptides were hydrolyzed with much higher catalytic efficiencies. In particular, the catalytic efficiencies for the hydrolysis of myristoyl peptide were more than 300-fold higher than that for the hydrolysis of acetyl peptide. The K_m value for the myristoyl peptide was lower than 1 μM (PfSir2A was saturated with 2 μM of the myristoyl peptide. The K_m value could not be accurately determined because of the detection limit at low substrate concentrations). The enzymology data demonstrated that PfSir2A preferentially hydrolyzes medium and long chain fatty acyl lysine.

Table 3. Kinetics data for PfSir2A on different acyl peptides

substrate	k_{cat} (s^{-1})	K_m **for peptide** (μM)	k_{cat}/K_m ($s^{-1}M^{-1}$)
H3K9 acetyl	0.001 ± 0.0002	39 ± 9	2.6×10^1
H3K9 butyryl	0.001 ± 0.0002	8 ± 1	1.6×10^2
H3K9 octanoyl	0.001 ± 0.004	1.2 ± 0. 3	9.2×10^2
H3K9 myristoyl	0.01± 0.002	<1.0[a]	$>1.0 \times 10^4$

a. The K_m value cannot be accurately determined due to the detection limit when substrate concentration was lower than 1 μM.

A

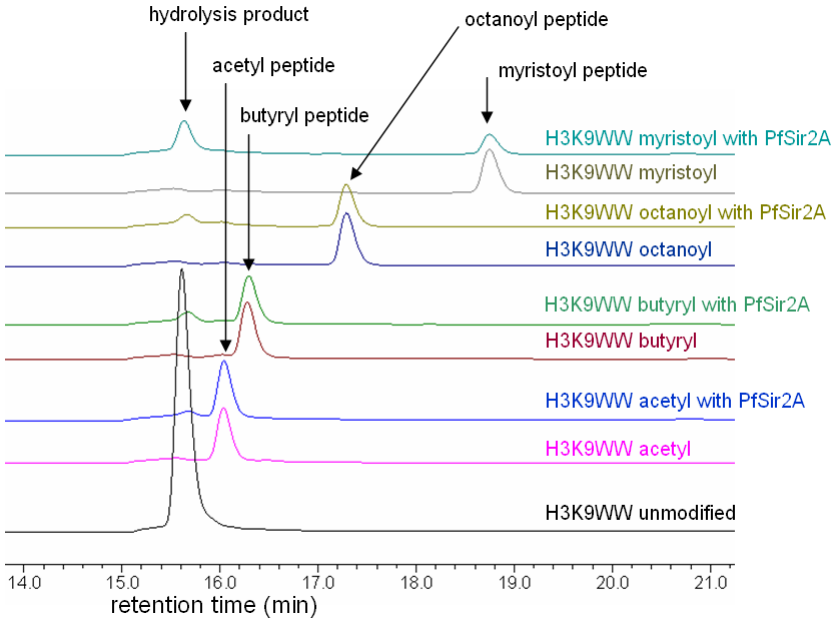

B

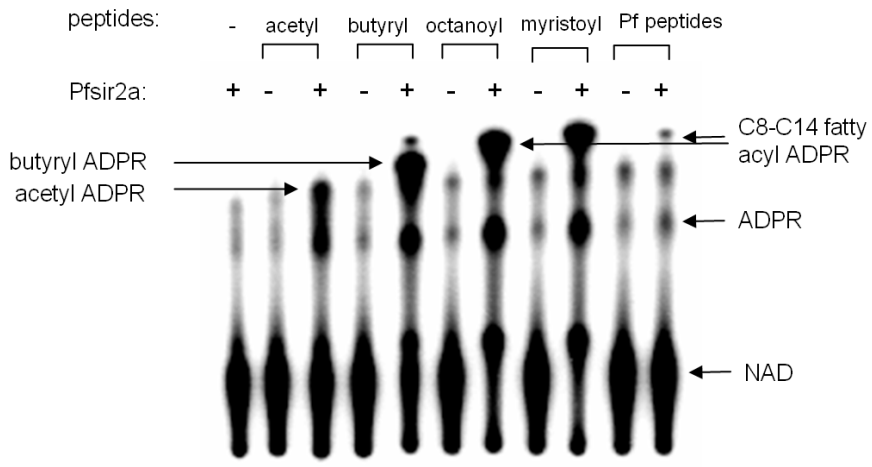

Figure 10. PfSir2A could hydrolyze medium and long chain fatty acyl lysine more efficiently than acetyl lysine. (a) Overlaid HPLC traces showing PfSir2A-catalyzed hydrolysis of different fatty acyl lysine peptides. Acyl peptides were used at 20 µM, PfSir2A at 1 µM, and NAD at 500 µM. The corresponding synthetic peptide without any acyl lysine modification (H3K9WW unmodified) was used as the control to indicate the position of the hydrolysis product formed. (b) ^{32}P-NAD assay could detect the presence of medium or long chain fatty acyl lysine modifications on *P. falciparum* proteins. PfSir2A were incubated with ^{32}P-NAD and synthetic peptides bearing different acyl modifications. Negative controls were reactions without PfSir2A or peptides. The reactions were resolved by TLC and detected by autoradiography. With *P. falciparum* peptides (last two lanes), the acyl ADPR spot formed was similar to the C8-C14 acyl ADPR, suggesting that such fatty acyl groups were present and could be removed by PfSir2A.

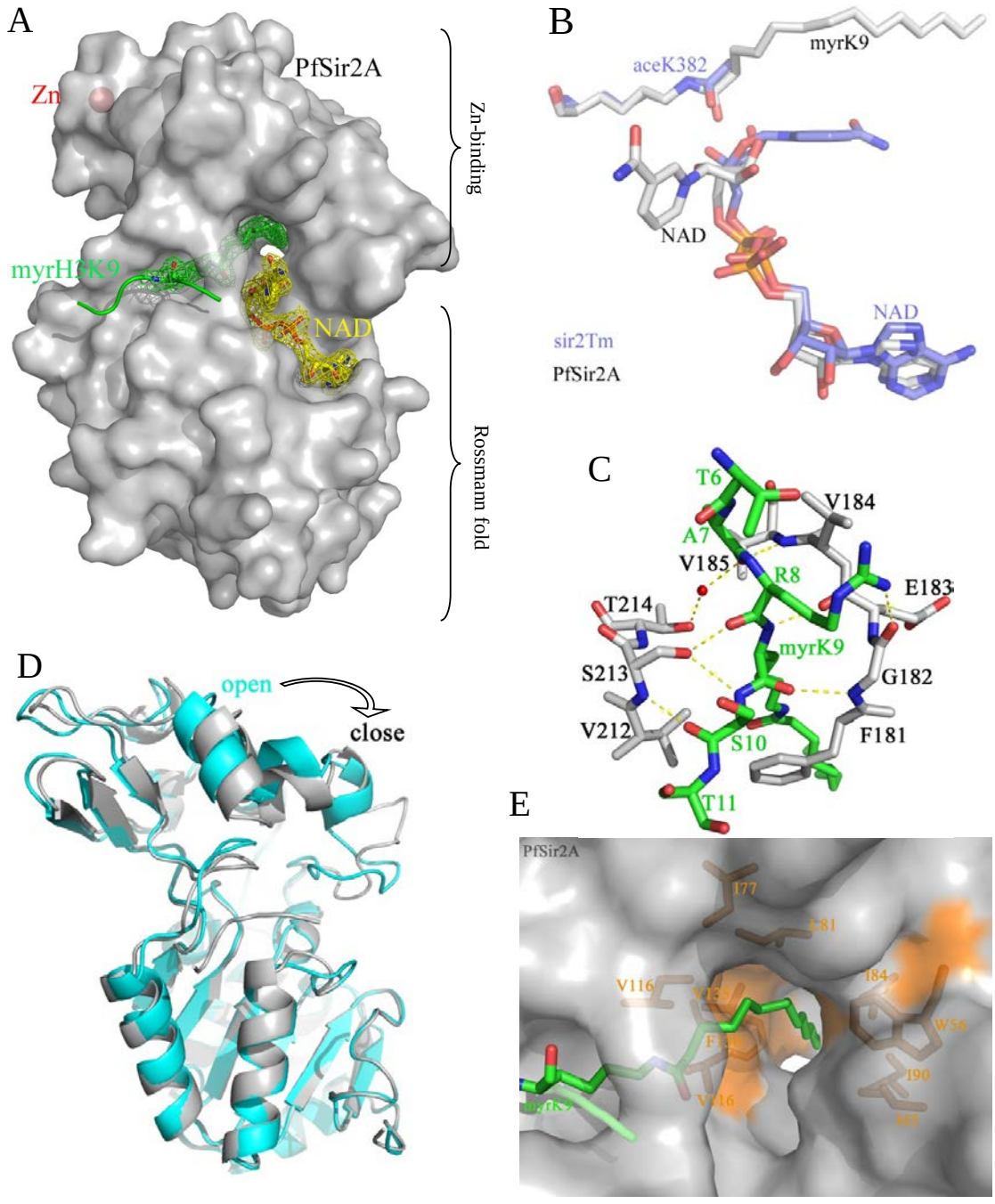

Figure 11. Structural basis for the recognition of myristoyl lysine by PfSir2A. (a) Overall structure of PfSir2A. The Fo-Fc map at 1.6σ shows the H3K9 myristoyl peptide (green) and NAD (yellow) at the active site. (b) The structural alignment between Sir2Tm (blue) and PfSir2A (grey). The positions of H3K9 myristoyl peptide and NAD in PfSir2A were similar to the positions of acetyl peptide and NAD in Sir2Tm. (c) Hydrogen bonding interactions between the H3K9 myristoyl peptide (green) and PfSir2A (grey). (d) Structural alignment between PfSir2A-AMP (cyan, PDB code: 3JWP) and PfSir2A-myrH3K9 showed that the binding of the substrate peptide myrH3K9 drove PfSir2A from an inactive open state to an active close state. (e) PfSir2A had a long open hydrophobic tunnel which accommodated fatty acyl groups. PfSir2A surface representation: grey; myristoyl lysine: green; hydrophobic residues: orange.

To understand the structural basis for PfSir2A' preference for longer chain fatty acyl groups, we co-crystallized PfSir2A with an H3K9 myristoyl peptide to generate the PfSir2A-H3K9 myristoyl complex. The co-crystal was then soaked briefly in an NAD solution to obtain a ternary complex of PfSir2A with H3K9 myristoyl peptide and NAD. The structures were solved using molecular replacement with the deposited PfSir2A structure PDB 3JWP as the search model. The overall structure of PfSir2A was similar to other sirtuins, containing a small Zn-binding domain and a large Rossmann fold domain (Fig.11a) [43-46]. The two substrates, H3K9 myristoyl peptide and NAD, bound to the clefts between the two domains. This binding mode of the two substrates was similar with the reported ternary complex structures of other sirtuins. For instance, the peptide substrates of the *Thermotoga maritima* Sir2 (Sir2Tm, PDB 2H4F, one of the first sirtuin ternary complex structureswith both NAD and acetyl peptide bound) and PfSir2A superimposed well (Fig. 11b) [47]. The interactions between PfSir2A and H3K9 myristoyl peptide mainly came from main chain hydrogen bonds (Fig. 11c), in agreement with other studies of sirtuins [47]. Compared with the structure without any acyl peptide bound (PDB 3JWP), the binding of H3K9 myristoyl peptide to PfSir2A caused the Zn-binding domain to rotate clockwise to the Rossmann fold domain, so that PfSir2A moved from an open state to a close state which is similar to that observed in Sir2Tm (Fig. 11d) [47]. However, different from Sir2Tm, PfSir2A had a long open hydrophobic tunnel that accommodated the myristoyl group (Fig.11e). The hydrophobic tunnel was surrounded by several hydrophobic residues (Ile45, Trp56, Ile77, Ile80, Ile84, Ile90, Val116, Val135, Phe136, Ile178, and Leu181). This structure feature suggested that PfSir2A was optimized for recognizing fatty acyl groups.

The enzymology and structural data led to the hypothesis that PfSir2A may function to remove medium and long chain fatty acyl groups in malaria parasite. Protein lysine

myristoylation has been reported to occur on several mammalian proteins [48, 49]. To test whether malaria parasite proteins have medium or long chain fatty acyl modifications on lysine residues, a sensitive assay was developed to detect the presence of fatty acyl lysine in malaria parasites. With the use of ^{32}P-NAD, the formation of fatty acylated ADP-ribose (ADPR) in PfSir2A-catalyzed defatty acylation of synthetic acyl peptides can be detected after thin-layer chromatography (TLC) separation and autoradiography. Longer chain fatty acyl ADPR species were more hydrophobic and thus moved faster than shorter chain fatty acyl ADPR species (Fig. 10b). Notably, most NAD molecules were consumed when octanoyl and myristoyl peptides were incubated with PfSir2A, while there were still NAD molecules left when acetyl and butyryl peptides were incubated with PfSir2A. This observation confirmed the kinetic studies that octanoyl and myristoyl peptides were more efficient substrate for PfSir2A. When total protein extracts of malaria parasites were incubated with ^{32}P-NAD and PfSir2A, the formation of a longer chain fatty acyl ADPR was detected. The position of the fatty acyl ADPR was similar to that formed the reactions with synthetic octanoyl and myristoyl peptides, suggesting that fatty acyl group on *P. falciparum* proteins should have a similar chain length. The intensity of the fatty acyl ADPR spot was weak, suggesting that the concentration of the fatty acyl peptide in our *P. falciparum* protein extract was low. However, we could repeatedly detect this spot using the ^{32}P-NAD assay. In addition, compared with the negative control without PfSir2A, the intensity for the acetyl ADPR spot did not increase. Therefore, PfSir2A's deacetylase activity could not be detected using *P. falciparum* protein extract, but the activity of removing longer fatty acyl groups could be detected.

In summary, our enzymology and structural data demonstrated that PfSir2A was more efficient at removing medium and long chain fatty acyl groups than acetyl groups from peptides.

Although it is known that other sirtuins can also hydrolyze propionyl and butyryl lysine, but the activity is typically weaker than the hydrolysis of acetyl lysine [50, 51]. Therefore, our work demonstrates for the first time that longer fatty acyl lysines can be the preferred substrate for a sirtuin. The biochemical data suggest that *P. falciparum* proteins contain such fatty acyl lysine modifications, which can be removed by PfSir2A *in vitro*. The data imply that the biological function of PfSir2A may be achieved by its activity of removing medium and long chain fatty acyl groups. The detailed structures of the fatty acyl groups and the abundance of such modifications in comparison to the well-known acetyl lysine modification await future studies. The finding that PfSir2A could remove longer fatty acyl groups suggests that other sirtuins, especially those that have weak or no deacetylase activity, may also have this activity. Sirtuins should therefore be called "NAD-dependent deacylases", instead of "NAD-dependent deacetylases". The discovery of a robust activity for PfSir2A will also facility the development of PfSir2 inhibitors, which may have therapeutic value in treating malaria.

METHODS

Cloning, expression, and purification of PfSir2A. PfSir2A gene was custom synthesized by Genscript. The sequence was codon optimized for overexpression in *E. coli* and cloned into pET-28a(+) vector with BamHI and XhoI restriction sites. The PfSir2A expression vector was then introduced into an *E. coli* BL21 with pRARE2. Successful transformants were selected by plating the cells on kanamycin (50 mg mL^{-1}) and chloramphenicol (20 mg mL^{-1}) luria broth (LB) plates. Single colonies were selected and grown in LB with kanamycin (50 mg mL^{-1}) and chloramphenicol (20 mg mL^{-1}) overnight at 37^{o}C. On the following day the cells were then subcultured (1:1000 (v/v)) into a 2 L LB with kanamycin (50 mg mL^{-1}) and chloramphenicol (20 mg mL^{-1}). The cells were induced with 500 μM of isopropyl β-D-1-thiogalactopyranoside (IPTG) at OD_{600} of 0.6 and grown overnight at 15^{o}C, 200 rpm. The cells were harvested by centrifugation at 6000 rpm for 10 minutes at 4^{o}C (Beckman Coulter Refrigerated Floor Centrifuge) and passed through an EmulsiFlex-C3 cell disruptor (AVESTIN, Inc.) 3 times. Cellular debris was removed by centrifuging at 20000 rpm for 30 minutes at 4^{o}C (Beckman Coulter). The PfSir2A was then purified using gravity flow Ni-affinity chromatography (Sigma) and dialyzed into 25 mM Tris pH 8.0, 50 mM NaCl, 1 mM DTT, 10% (v/v) glycerol. The proteins were then aliquoted and kept frozen at -80^{o}C. For crystallization, the 6-His tag of PfSir2A was removed by overnight incubation at 4°C with 30 unit mL^{-1} of thrombin (Haematologic Technologies Inc.), followed by Ni-affinity column purification to separate the undigested PfSir2A from the digested one. Then, the tag-free PfSir2A was further purified by FPLC with Superdex^{TM} 75 column (Bio-rad), dialyzed into crystallization buffer (20 mM HEPES, pH 7.1, 20 mM NaCl, 5 mM DTT, 3% (v/v) glycerol), concentrated into 10 mg mL^{-1}, flash frozen by liquid nitrogen, and stored at -80 °C for crystallization.

Synthesis of acyl peptides. Solvents were purchased from Fisher Scientific unless otherwise specified and peptide synthesis reagents and Fmoc-protected amino acids and derivatives were purchased from Creosalus Inc.

The H3K9 (NH_2-KQTARK*STGGWW-COOH) backbone was prepared using standard solid phase peptide synthesis (SPPS) at room temperature (RT). Wang resins SS (100-200 mesh, 1% DVB, 10 mmole/g) were placed into a peptide synthesis vessel along with 5 mL of anhydrous dichloromethane (DCM) for 5 hours. The first activated amino acid solution was freshly prepared with 0.32 mmoles of Fmoc-W-OH, 0.32 mmoles of O-benzotriazole-*N*,*N*,*N'*,*N'*-tetramethyl-uronium-hexafluoro-phosphate (HBTU), 0.133 mmoles of 4-dimethylaminopyridine (DMAP), 0.64 mmoles of diisopropylethylamine (DIEA, added last) and an appropriate amount of anhydrous *N*,*N'*-dimethylformamide (DMF). The resin was incubated with the solution overnight at RT. The resins were then washed with DMF (5 times) before incubating with a cocktail of acetic anhydride, pyridine and DMF (2:1:3 ratio (v/v)) for 30 minutes to block remaining amino groups on the resin. Kaiser test was used to test the success of the coupling. Once coupling was confirmed, 20% (v/v) piperidine in DMF was used to remove Fmoc. All subsequent activated amino acid derivatives were freshly prepared with 0.24 mmoles of the amino acid, 0.24 mmole of HBTU, 0.21 mmole of N-hydroxybenzotriazole (HOBT), 0.48 mmole of DIEA in DMF and reaction time was 2 hours at RT.

The lysine to be modified by different acyl groups (K*) was protected with allyl carbamate (Alloc) on the side chain while the N-terminal K was protected by Boc. After all the peptide coupling steps were done on the resin, the Alloc group was removed by incubating the resin in a cocktail of DCM, morpholine (Sigma, 2.5%) and glacial acetic acid (5%) with a 1:1 weight ratio of the original resin and tetrakis(triphenylphosphine)palladium(0) for 4 hours under nitrogen.

Several washes of 0.5% (v/v) DIEA in DCM and 0.02 M of diethyldicarbamate in DMF were carried out to remove the palladium. The resin was then incubated with solutions for putting on different acyl groups. The acylation solutions contained 0.24 mmoles of fatty acids of different chain lengths (acetic anhydride, butyric acid, octanoic acid, or myristic acid), 0.24 mmole of HBTU, 0.21 mmole of HOBT, 0.48 mmole of DIEA and DMF. The resin was then washed with DMF and the peptides were cleaved with a mixture of trifluoroacetic acid (TFA), 5% (v/v) water, 5% (w/v) phenol, 2.5% (v/v) ethanedithiol and 5% (v/v) thioanisole. TFA was removed from the filtered peptide solution and the peptides were precipitated out by the addition of ether and lyophilized. The crude peptides were dissolved in water and purified by HPLC (Beckman Coulter System Gold 125P solvent module and 168 Detector) using a TARGA C18 column (250 x 20 mm, 10 μM, Higgins Analytical, Inc.) with mobile phase A (water with 0.1% (v/v) TFA) and B (acetonitrile with 0.1% (v/v) TFA) at a gradient of 20% B to 100% B in 50 minutes and a flow rate of 10 mL/min. The peptides were monitored at 215 nm and 280 nm and fractions were collected. LCMS (SHIMADZU LCMS-QP8000α with a Sprite TARGA C18 column (40 × 2.1 mm, 5 μm, Higgins Analytical, Inc.) was used to confirm the peptide mass and high purity fractions were lyophilized. The solvents used in LCMS were water with 0.1% (v/v) formic acid and acetonitrile with 0.1% (v/v) formic acid.

HPLC assay and kinetics. Activity of PfSir2A was determined using HPLC, by quntifying the modified and unmodified H3K9 peptide. The reaction contained 20 mM of Tris pH 8.0, 1 mM DTT, 20 μM H3K9 modified peptide, 1 mM of NAD and 1 μM of PfSir2A and was incubated at 37^{o}C for 1 hour. The reaction was quenched with 1 volume of 10% (v/v) TFA and spun down for 10 minutes at 18,000 g (Beckman Coulter Microfuge) to separate the PfSir2A from the reaction. The supernatant was then analyzed by HPLC.

The k_{cat} and K_m values were determined using HPLC to quantify the amount of product formed with varying concentrations of the modified peptide with 1 mM of NAD, 20 mM Tris pH 8.0, 50 mM DTT, 0.5 μM of PfSir2A (butyryl, octanoyl and myristoyl H3K9 peptide), and 1 μM of PfSir2A was used for acetyl H3K9. Peptide concentration used for H3K9 acetyl and butyryl were both 2, 4, 8, 16, 32, 64, 128, and 256 μM with an incubation time of 40 and 20 minutes, respectively. Peptide concentration used for H3K9 octanoyl was 1, 2, 4, 8, 16, 32, 64, and 128 μM with an incubation time of 15 minutes. Peptide concentration used for H3K9 myristoyl was 1, 2, 3, 4, 5, 6, 8, and 16 μM with an incubation time of 1 minute. The stock solutions of the different peptides were made in different solvents. H3K9 acetyl was stored in water while the longer fatty acyl peptides, butyryl and octanoyl were stored in 1:1 (v/v) DMSO:water solutions. The myristoyl peptide is especially hydrophobic and was stored in DMSO. If only water was used to dissolve them, the peptides would stick to the plastic tubes used and led to errors in the peptide concentration. The final concentrations of DMSO in the assays varied from 0 to 10% by volume. The quenched reactions were then analyzed via HPLC using a reverse phase analytical column (Sprite TARGA C18, 40 × 2.1 mm, 5 μm, Higgins Analytical, Inc.) with a 0% to 70% B gradient in 8 minutes at 1 mL/min. The acetyl peptide has a very close retention time to the unmodified peptide and a different column was used to separate the peaks (Kinetex XB-C18 100A, 75x 4.60 mm, 2.6 um, Phenomenex). The product peak and the substrate peaks were both quantified and converted to initial rates, which were then plotted against the modified peptide concentration and fitted using the Kaleidagraph program.

^{32}P-NAD assay. The reaction contained 50 mM Tris pH 8.0, 150 mM NaCl, 10 mM DTT, 60 μM H3K9 modified peptide, 0.1 μCi of ^{32}P-NAD (American Radiolabeled Chemicals, ARP 0141-250 μCi) and 1 μM of Pfsir2A and was incubated at 37^{o}C for 1 hour.

P. falciparum whole cell lysate (100 μL) was first denatured with 6 M of Urea, 15 mM of DTT at 37^{o}C for 15 minutes. Then it was alkylated with 50 mM of iodoacetamide in the dark at RT for 1 hour. The solution was then diluted so that the final concentration of urea was less than 0.75 M and digested with 0.1 μg/μL trypsin and 50 mM Tris pH 7.4, and 1 mM $CaCl_2$ overnight at 37^{o}C. The digest was quenched with 10% (v/v) TFA to a final pH of 2 to 3 and desalted with a Waters C18 Sep-Pak column. The peptides were eluted 5 times with 1 mL of 90% (v/v) ACN/0.1% (v/v) TFA and lyophilized. The peptides were then solubilized in 50 μL of water and 1 μL was used in the ^{32}P-NAD assay under conditions described above. The reaction was incubated at 37^{o}C for 15 minutes and 1 μL of the reaction mixture was spotted onto a polyester backed silica plate (100 μm thick, Waters). After the spots were dried, the plate was run for 6 cm in 30:70 (v/v) 1M ammonium bicarbonate: 95% ethanol. The plate was dried and exposed overnight in a PhosphorImaging screen (GE Healthcare). The signal was detected using a STORM860 phosphorimager (GE Healthcare).

Crystallization, data collection, and structural refinement. PfSir2A was mixed with H3K9 myristoyl peptide at the protein:peptide ratio of 1:10, diluted into 3 mg mL^{-1} with crystallization buffer, and incubated on ice for 30-60 minutes. Crystals were grown at room temperature with hanging drop vapor diffusion method at the condition of 16% PEG 3350, 0.1 M NaF, 7% formamide. PfSir2A-H3K9 myristoyl co-crystals were soaked in the cryoprotectant solution (18% PEG 3350, 0.1 M NaF, 10% formamide, 15% glycerol) with 10 mM NAD for 2-10 minutes at room temperature immediately before data collection. All data were collected at CHESS (Cornell High Energy Synchrotron Source) F2 station. The data were processed using the programs HKL2000 [52]. Using the program Molrep from the CCP4 suite of programs [53], the structures were solved by molecular replacement with PfSir2A-AMP structure (PDB code:

3JWP) as the searching template. Refinement and model building were performed with REFMAC5 and COOT from CCP4. The X-ray diffraction data collection and structure refinement statistics were shown in Table 4.

Table 4. Crystallographic Data Collection and Refinement Statistics

	PfSir2A_myrH3K9	PfSir2A-myrH3K9-NAD
Data collection		
Space group	$P2_12_12$	$P2_12_12$
Cell dimensions		
a, *b*, *c* (Å)	32.51, 103.33, 105.51	32.17, 102.73, 105.18
α, β, γ (°)	90, 90, 90	90, 90, 90
Resolution (Å)	50-2.40	50-2.20
R_{sym} or R_{merge} (%)	14.9 (75.3)	12.9 (74.8)
$I / \sigma I$	23.83 (1.75)	24.7 (2.21)
Completeness (%)	98.5 (97.2)	99.9 (99.9)
Redundancy	8.2 (4.4)	6.7 (5.0)
Refinement		
Resolution (Å)	50-2.40	50-2.20
No. reflections	18972	23688
R_{work} / R_{free} (%)	21.59 /27. 00	20.38/25.03
No. of protein residues	263	271
No. of ligand/ion molecules		
Myristoyl H3K9	1	1
NAD	--	1
Glycerol	1	1
Zn	1	1
No. of water	26	78
R.m.s deviations		
Bond lengths (Å)	0.039	0.020
Bond angles (°)	2.18	1.93

Numbers showed in the parentheses are for the highest resolution shell.

Acknowledgement. This work is supported in part by NIH R01GM086703 (H.L.), NIH RR01646 (Q.H.) and Hong Kong GRF766510 (Q.H.). A.Y.Z. is a CBI training grant trainee (NIH T32 GM08500).

CONCLUDING REMARKS

Our aim was to verify the importance of the two conserved residues in type III sirtuins and investigate the physiological significance of these new post translational modifications in a bacterial model. We investigated the activity of two sirtuins, *E. coli* CobB and *P. falciparum* Sir2A (PfSir2A). CobB contains the two active site residues, Tyr and Arg, that are conserved in most class III sirtuins, while PfSir2A does not have the Tyr and Arg residues even though it is classified as a class III sirtuin. We found that only CobB has desuccinylase activity while PfSir2A prefers to remove long fatty acyl chains. This finding further confirms the importance of the Tyr and Arg residues in recognizing negatively charged acyl groups, such as succinyl and malonyl. Interestingly, CobB is multifunctional sirtuin that can remove both acetyl and succinyl efficiently. We also investigated CobB's influence on metabolism in different nutrient conditions and found that desuccinylation was not important in acetate, succinate and propionate supplemented nutrients.

REFERENCES

1. Frye, R.A., *Phylogenetic classification of prokaryotic and eukaryotic Sir2-like proteins.* Biochem Biophys Res Commun, 2000. **273**(2): p. 793-8.
2. Verdin, E., *Histone deacetylases : transcriptional regulation and other cellular functions*. Cancer drug discovery and development2006, Totowa, N.J.: Humana Press. xi, 340 p.
3. Frye, R.A., *Characterization of five human cDNAs with homology to the yeast SIR2 gene: Sir2-like proteins (sirtuins) metabolize NAD and may have protein ADP-ribosyltransferase activity.* Biochem Biophys Res Commun, 1999. **260**(1): p. 273-9.
4. Morris, B.J., *Seven sirtuins for seven deadly diseases of aging.* Free Radic Biol Med, 2012.
5. Hawse, W.F. and C. Wolberger, *Structure-based mechanism of ADP-ribosylation by sirtuins.* J Biol Chem, 2009. **284**(48): p. 33654-61.
6. Du, J., H. Jiang, and H. Lin, *Investigating the ADP-ribosyltransferase activity of sirtuins with NAD analogues and 32P-NAD.* Biochemistry, 2009. **48**(13): p. 2878-90.
7. Kowieski, T.M., S. Lee, and J.M. Denu, *Acetylation-dependent ADP-ribosylation by Trypanosoma brucei Sir2.* J Biol Chem, 2008. **283**(9): p. 5317-26.
8. He, W., et al., *Mitochondrial sirtuins: regulators of protein acylation and metabolism.* Trends Endocrinol Metab, 2012.
9. Zhang, J., et al., *Lysine acetylation is a highly abundant and evolutionarily conserved modification in Escherichia coli.* Mol Cell Proteomics, 2009. **8**(2): p. 215-25.
10. Yu, B.J., et al., *The diversity of lysine-acetylated proteins in Escherichia coli.* J Microbiol Biotechnol, 2008. **18**(9): p. 1529-36.
11. Starai, V.J. and J.C. Escalante-Semerena, *Identification of the protein acetyltransferase (Pat) enzyme that acetylates acetyl-CoA synthetase in Salmonella enterica.* J Mol Biol, 2004. **340**(5): p. 1005-12.
12. Yan, J., et al., *In vivo acetylation of CheY, a response regulator in chemotaxis of Escherichia coli.* J Mol Biol, 2008. **376**(5): p. 1260-71.
13. Hu, L.I., B.P. Lima, and A.J. Wolfe, *Bacterial protein acetylation: the dawning of a new age.* Mol Microbiol, 2010. **77**(1): p. 15-21.
14. Thao, S., et al., *Nepsilon-lysine acetylation of a bacterial transcription factor inhibits Its DNA-binding activity.* PLoS One, 2010. **5**(12): p. e15123.
15. Yu, J. and J. Auwerx, *The role of sirtuins in the control of metabolic homeostasis.* Ann N Y Acad Sci, 2009. **1173 Suppl 1**: p. E10-9.
16. Du, J., et al., *Sirt5 is a NAD-dependent protein lysine demalonylase and desuccinylase.* Science, 2011. **334**(6057): p. 806-9.
17. Bao, J. and M.N. Sack, *Protein deacetylation by sirtuins: delineating a post-translational regulatory program responsive to nutrient and redox stressors.* Cell Mol Life Sci, 2010. **67**(18): p. 3073-87.
18. Zhao, S., et al., *Regulation of Cellular Metabolism by Protein Lysine Acetylation.* Science, 2010. **327**(5968): p. 1000-1004.
19. Wang, Q., et al., *Acetylation of metabolic enzymes coordinates carbon source utilization and metabolic flux.* Science, 2010. **327**(5968): p. 1004-1007.

20. Bohm, L., et al., *Influence of histone acetylation on the modification of cytoplasmic and nuclear proteins by ADP-ribosylation in response to free radicals.* Biochim Biophys Acta, 1997. **1334**(2-3): p. 149-54.
21. Danilova, A.B. and L.N. Grinkevich, *Failure of long-term memory formation in juvenile snails is determined by acetylation status of histone H3 and can be improved by NaB treatment.* PLoS One, 2012. **7**(7): p. e41828.
22. Tucker, A.C. and J.C. Escalante-Semerena, *Biologically active isoforms of CobB sirtuin deacetylase in Salmonella enterica and Erwinia amylovora.* J Bacteriol, 2010. **192**(23): p. 6200-8.
23. Garrity, J., et al., *N-Lysine Propionylation Controls the Activity of Propionyl-CoA Synthetase.* J. Biol. Chem., 2007. **282**(41): p. 30239-30245.
24. Li, R., et al., *CobB regulates Escherichia coli chemotaxis by deacetylating the response regulator CheY.* Mol Microbiol, 2010. **76**(5): p. 1162-74.
25. Zhang, Z., et al., *Identification of lysine succinylation as a new post-translational modification.* Nat Chem Biol, 2011. **7**(1): p. 58-63.
26. Blanco-Garcia, N., et al., *Autoacetylation regulates P/CAF nuclear localization.* J Biol Chem, 2009. **284**(3): p. 1343-52.
27. Black, J.C., et al., *The SIRT2 deacetylase regulates autoacetylation of p300.* Mol Cell, 2008. **32**(3): p. 449-55.
28. Bansal, S., et al., *Autoacetylation of purified calreticulin transacetylase utilizing acetoxycoumarin as the acetyl group donor.* Appl Biochem Biotechnol, 2009. **157**(2): p. 285-98.
29. Arif, M., et al., *Autoacetylation induced specific structural changes in histone acetyltransferase domain of p300: probed by surface enhanced Raman spectroscopy.* J Phys Chem B, 2007. **111**(41): p. 11877-9.
30. Imai, S.-i., et al., *Transcriptional silencing and longevity protein Sir2 is an NAD-dependent histone deacetylase.* Nature, 2000. **403**(6771): p. 795-800.
31. Sauve, A.A., et al., *The biochemistry of sirtuins.* Annu. Rev. Biochem., 2006. **75**: p. 435-465.
32. Imai, S.-i. and L. Guarente, *Ten years of NAD-dependent SIR2 family deacetylases: implications for metabolic diseases.* Trends in Pharmacological Sciences, 2010. **31**(5): p. 212-220.
33. Haigis, M.C. and D.A. Sinclair, *Mammalian Sirtuins: Biological Insights and Disease Relevance.* Annu. Rev. Pathol., 2010. **5**(1): p. 253-295.
34. Frye, R.A., *Phylogenetic classification of prokaryotic and eukaryotic Sir2-like proteins.* Biochem. Biophys. Res. Commun., 2000. **273**(2): p. 793-798.
35. Freitas-Junior, L.H., et al., *Telomeric heterochromatin propagation and histone acetylation control mutually exclusive expression of antigenic variation genes in malaria parasites.* Cell, 2005. **121**(1): p. 25-36.
36. Tonkin, C.J., et al., *Sir2 paralogues cooperate to regulate virulence genes and antigenic variation in Plasmodium falciparum.* PLoS Biol., 2009. **7**(4): p. e1000084.
37. Merrick, C.J. and M.T. Duraisingh, *Plasmodium falciparum Sir2: an Unusual Sirtuin with Dual Histone Deacetylase and ADP-Ribosyltransferase Activity.* Eukaryotic Cell, 2007. **6**(11): p. 2081-2091.

38. French, J.B., Y. Cen, and A.A. Sauve, *Plasmodium falciparum Sir2 is an NAD^+-dependent deacetylase and an acetyllysine-dependent and acetyllysine-independent NAD^+ glycohydrolase.* Biochemistry, 2008. **47**(38): p. 10227-10239.
39. Kowieski, T.M., S. Lee, and J.M. Denu, *Acetylation-dependent ADP-ribosylation by Trypanosoma brucei Sir2.* J. Biol. Chem., 2008. **283**(9): p. 5317-5326.
40. Du, J., H. Jiang, and H. Lin, *Investigating the ADP-ribosyltransferase activity of sirtuins with NAD analogs and ^{32}P-NAD.* Biochemistry, 2009. **48**: p. 2878-2890.
41. Chen, Y., et al., *Lysine propionylation and butyrylation are novel post-translational modifications in histones.* Mol. Cell. Proteomics, 2007. **6**(5): p. 812-819.
42. Liu, B., et al., *Identification and characterization of propionylation at histone H3 lysine 23 in mammalian cells.* J. Biol. Chem., 2009. **284**(47): p. 32288-32295.
43. Finnin, M.S., J.R. Donigian, and N.P. Pavletich, *Structure of the histone deacetylase SIRT2.* Nat. Struct. Mol. Biol., 2001. **8**(7): p. 621-625.
44. Zhao, K., et al., *Structure and autoregulation of the yeast Hst2 homolog of Sir2.* Nat Struct Mol Biol, 2003. **10**(10): p. 864-871.
45. Avalos, J.L., et al., *Structure of a Sir2 enzyme bound to an acetylated p53 peptide.* Mol. Cell, 2002. **10**(3): p. 523-535.
46. Min, J., et al., *Crystal structure of a SIR2 homolog-NAD complex.* Cell, 2001. **105**(2): p. 269-279.
47. Hoff, K.G., et al., *Insights into the sirtuin mechanism from ternary complexes containing NAD^+ and acetylated peptide.* Structure, 2006. **14**(8): p. 1231-1240.
48. Stevenson, F.T., et al., *Myristyl acylation of the tumor necrosis factor alpha precursor on specific lysine residues.* J. Exp. Med., 1992. **176**(4): p. 1053-1062.
49. Stevenson, F.T., et al., *The 31-kDa precursor of interleukin 1 alpha is myristoylated on specific lysines within the 16-kDa N-terminal propiece.* Proc. Natl. Acad. Sci. U. S. A., 1993. **90**(15): p. 7245-7249.
50. Smith, B.C. and J.M. Denu, *Acetyl-lysine Analog Peptides as Mechanistic Probes of Protein Deacetylases.* J. Biol. Chem., 2007. **282**(51): p. 37256-37265.
51. Bheda, P., et al., *Structure of Sir2Tm bound to a propionylated peptide.* Protein Science, 2011. **20**(1): p. 131-139.
52. Otwinowski, Z. and W. Minor, *Processing of X-ray diffraction data collected in oscillation mode.* Methods Enzymol., 1997. **276**: p. 472-494.
53. Collaborative, *The CCP4 suite: programs for protein crystallography.* Acta Crystallogr. D Biol. Crystallogr., 1994. **50**(5): p. 760-763.

Title: Plasmodium falciparum Sir2A Preferentially Hydrolyzes Medium and Long Chain Fatty Acyl Lysine

Author: Anita Y. Zhu, Yeyun Zhou, Saba Khan, Kirk W. Deitsch, Quan Hao, and Hening Lin

Publication: ACS Chemical Biology

Publisher: American Chemical Society

Date: Jan 1, 2012

PERMISSION/LICENSE IS GRANTED FOR YOUR ORDER AT NO CHARGE

This type of permission/license, instead of the standard Terms & Conditions, is sent to you because no fee is being charged for your order. Please note the following:

- Permission is granted for your request in both print and electronic formats, and translations.
- If figures and/or tables were requested, they may be adapted or used in part.
- Please print this page for your records and send a copy of it to your publisher/graduate school.
- Appropriate credit for the requested material should be given as follows: "Reprinted (adapted) with permission from (COMPLETE REFERENCE CITATION). Copyright (YEAR) American Chemical Society." Insert appropriate information in place of the capitalized words.
- One-time permission is granted only for the use specified in your request. No additional uses are granted (such as derivative works or other editions). For any other uses, please submit a new request.